Organic & Biomolecular Chemistry

PAPER

View Article Online
View Journal | View Issue

Open Access Article. Published on 07 June 2016. Downloaded on 11/1/2025 4:50:22 AM.
This article is licensed under a Creative Commons Attribution-NonCommercial 3.0 Unported Licence.

Cite this: *Org. Biomol. Chem.*, 2016, **14**, 6539

Synthesis and evaluation of influenza A viral neuraminidase candidate inhibitors based on a bicyclo[3.1.0]hexane scaffold†

Cinzia Colombo,[a,b] B. Mario Pinto,[a] Anna Bernardi[b] and Andrew J. Bennet*[a]

Received 7th May 2016,
Accepted 7th June 2016

DOI: 10.1039/c6ob00999a

www.rsc.org/obc

This manuscript describes a novel class of derivatives based on a bicyclo[3.1.0]hexane scaffold, proposed as mimics of sialic acid in a distorted boat conformation that is on the catalytic pathway of neuraminidases (sialidases). A general synthetic route for these constrained-ring molecules was developed using a photochemical reaction followed by a Johnson–Corey–Chaykovsky cyclopropanation. Functionalization with the goal of occupying the 150-cavity was also exploited. Inhibition assays demonstrated low micromolar inhibition against both group-1 (H5N1) and group-2 (H9N2) influenza neuraminidase subtypes, indicating good affinity for the alpha and beta sialic acid mimics and 150-cavity-targeted derivatives. These results provide a validation of a bicyclo[3.1.0]hexane scaffold as a mimic of a distorted sialic acid bound in the neuraminidase active site during catalysis.

Introduction

Influenza neuraminidase (NA) is the enzyme expressed on the surface of the influenza virus that catalyzes the release of progeny virions from infected cells by cleaving the sialic acid receptor on host cells. Thus, it plays a fundamental role in the influenza infection process.[1] To date, the most successful anti-influenza drugs target NA activity. Fig. 1 shows oseltamivir **1**,[2] zanamivir **2**,[3] and peramivir **3**[4,5] that were developed based on the structure of sialic acid bound in the active site of NA. The emergence of resistant influenza NA strains, especially in the case of oseltamivir, underscores the growing demand for the development of new antiviral drugs with novel structural motifs and/or substitution patterns.[6]

Phylogenetically, the nine NA subtypes can be divided into two groups: group 1 (N1, 4, 5 and 8), and group 2 (N2, 3, 6, 7 and 9).[7] Structural characterization of various NAs led to the discovery of a potential binding pocket close to the active site, which was named the '150-cavity' because it is capped by a loop that contains residues 147–152 (150-loop).[7] That is, within structures of apo-enzymes the 150-loop was reported to adopt an open conformation in group 1 enzymes and a closed conformation for group 2 neuraminidases.[7]

Some recent inhibitors have tried to exploit contacts in this region to increase affinity.[8–10] The 150-cavity opens through the dynamics of residues 147–152 (the 150-loop). Movement of the 150-loop was initially thought to be restricted to group-1 NAs;[7] however, MD simulations[11–13] and crystallographic evidence of a partially open 150-loop in a group-2 NA[14] show the flexibility of this loop, which implies that all NAs may retain the propensity for opening the 150-loop (Fig. 2).

Recently, one of us reported a carbocyclic analogue of zanamivir in which the hydrophilic glycerol side chain is replaced with the 3-pentyloxy group of oseltamivir (**4**, Fig. 1) and a series of triazole-containing carbocycles to target both the catalytic site and the 150-cavity (**5–7**, Fig. 1).[10,15,16] Compounds **4** and **5** displayed a much stronger affinity for an N1 NA than an N2 enzyme.[15] Of note, second-generation oseltamivir-like compounds (**6** and **7**, Fig. 1), which reinstated the basic functionality on C-5, showed generally improved inhibition of virus replication in a cell-based assay, highlighting the importance of a basic group at C-5.[17] These molecules showed strong inhibition of the HK1 (H3N2) strain but a slightly lower activity towards the PR8 (H1N1) strain, supporting the notion that the 150-cavity could be opened in both NA groups. Several compounds were then designed to exploit contacts in this region by appending substituents at various positions. The 3-(4-toluoyl)allyl derivative (**8**, Fig. 1), for instance, inhibited several N1 strains more strongly than a N2 strain (A/Paris/908/97; H3N2).[8]

[a]*Department of Chemistry, Simon Fraser University, 8888 University Drive, Burnaby, British Columbia, Canada V5A 1S6. E-mail: bennet@sfu.ca; Fax: +1-778-782-3765; Tel: +1-778-782-8814*

[b]*Università degli Studi di Milano, Dipartimento di Chimica, Via Golgi 19, I-20133 Milano, Italy*

† Electronic supplementary information (ESI) available: Figures and tables containing ^{1}H and ^{13}C NMR spectra, kinetics data. See DOI: 10.1039/c6ob00999a

Open Access Article. Published on 07 June 2016. Downloaded on 11/1/2025 4:50:22 AM.
This article is licensed under a Creative Commons Attribution-NonCommercial 3.0 Unported Licence.

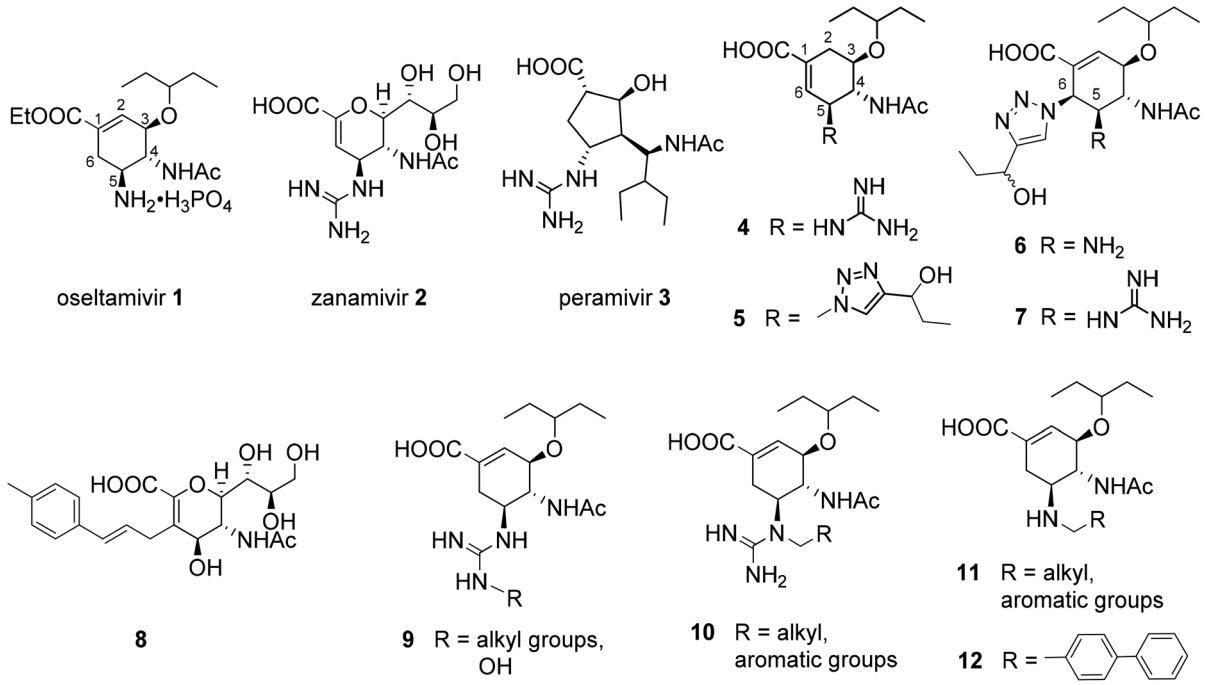

Fig. 1 Structure of oseltamivir **1**, zanamivir **2** and peramivir **3** and related compounds designed to target the NA 150-cavity.

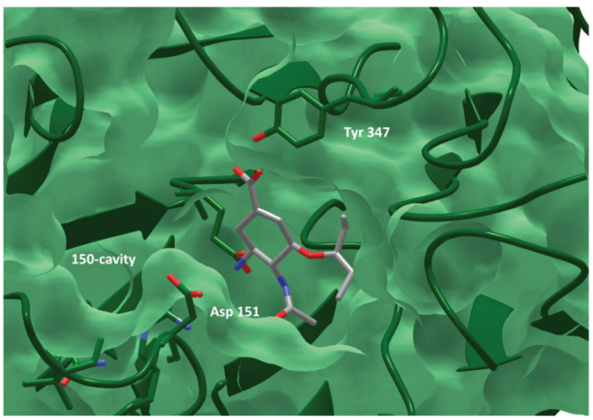

Fig. 2 Molecular surface of N1 neuraminidase with the free acid of oseltamivir **1** bound (source: pdb 2HU0). The 150-cavity is accessible due to an open 150-loop conformation (residues 147–152).

Oseltamivir analogues bearing *N*-substituted guanidines (compounds of general formula **9–10**, Fig. 1)[9,18] and amines (compounds of general formula **11**, Fig. 1)[9] have also been made and tested. Only relatively small substituents appended to a terminal guanidino nitrogen atom (**9**, *N*-methyl and *N*-hydroxyl) had a beneficial effect on the activity while bulkier substituents (**9**, R > CH_3) had a dramatically reduced activity.[18] Of note, several alkyl derivatives of compounds with the general structures **10** and **11** had improved activities.[9] While, *p*-phenylbenzyl amine **12** (Fig. 1) showed better IC_{50} values than oseltamivir carboxylate **1** against NAs from three H5N1 virus strains.[9] All of these inhibitors were designed based on an understanding of the mechanism of neuraminidases, which are retaining glycosidases. The accepted mechanism for neuraminidases (sialidases) involves formation of a glycosylated enzyme intermediate[19,20] in which both glycosylation and deglycosylation occur *via* transition states (TS) that have substantial oxacarbenium ion character and a distorted six-membered ring (Fig. 3).[21–23]

The introduction of a double bond into the carbohydrate six-membered ring changes the ground state conformation and has been used as a general strategy to try to mimic the geometry of the enzymatic TS.[2,10] Molecular modeling studies suggest that the Michaelis complex between N1 and substrate forces the pyran ring into a $^4S_2$ or a $B_{2,5}$ conformation,[24] whereas that in a bacterial sialidase complex has been proposed to be a $^6S_2$ skew-boat.[23] If the substrate is bound in a skew-boat conformation and the TS is located between the Michaelis complex and the enzyme-bound intermediate,[25] then the bicyclo[3.1.0] analogue **13** likely mimics the TS structure (Fig. 3).

Other conformationally restricted bicyclic compounds have been shown to be good glycosidase inhibitors.[26,27] Herein, we describe the synthesis and evaluation of compounds that incorporate a bicyclo[3.1.0]hexane, to provide the ring distortion required to mimic the TS (compounds **13–17**, Fig. 4). These possible transition state analogues, which contain a new structural motif, may display a reduced propensity for eliciting resistant strains. Inhibition studies of influenza A sialidases by **13–17** revealed interesting similarities with the more conformationally flexible phosphonate mimics of sialic acid **18** and **19** (Fig. 4), previously reported in the literature.[28]

 This journal is © The Royal Society of Chemistry 2016

Open Access Article. Published on 07 June 2016. Downloaded on 11/1/2025 4:50:22 AM.
This article is licensed under a Creative Commons Attribution-NonCommercial 3.0 Unported Licence.

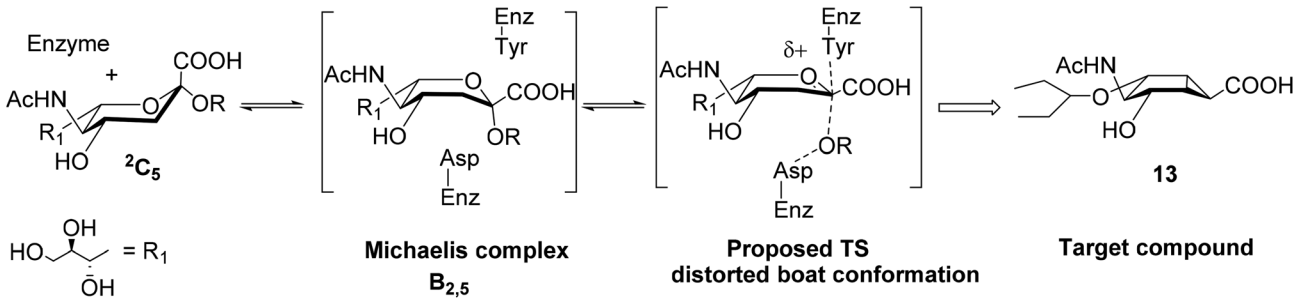

Fig. 3 Sialic acid ring distortion during catalysis and target compound described herein.

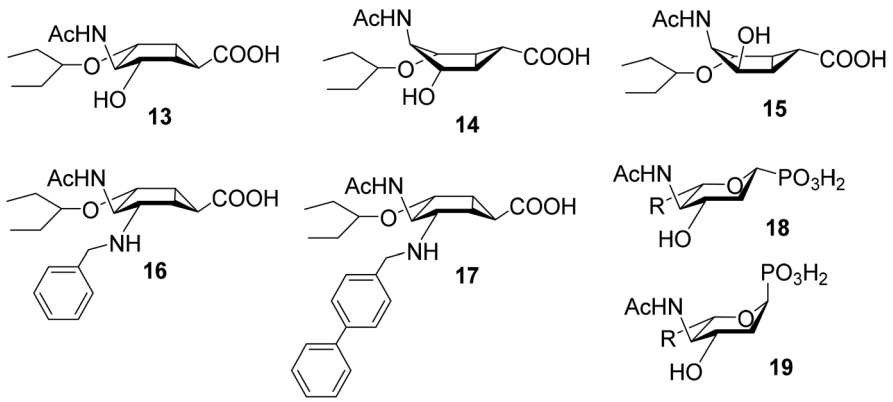

Fig. 4 Constrained sialic acid analogues (**13–17**) described in this manuscript and α- and β-phosphonate analogues **18** and **19**.[39] Bicyclo[3.1.0] hexanes are drawn in their intrinsically preferred boat-like conformation.

Results and discussion

Synthesis

Retrosynthetically, compound **13** can be made conveniently from pyridine, as shown in Scheme 1, through a photoinduced cyclization of a pyridinium cation with concomitant stereocontrolled nucleophile addition to produce aziridine **22**. Enone **21** could then be obtained by regioselective ring opening of aziridine **22** followed by protecting group manipulation. Finally, cyclopropanation of cyclopentenone **21** should generate the bicyclo[3.1.0] framework of **20**, which, after functional group interconversion and ester hydrolysis, should yield the bicyclo [3.1.0]hexane scaffold **13**.

The starting five-membered ring derivative **22** was indeed obtained through a photochemical reaction of the pyridinium cation **23** (Scheme 2).

Initially reported in 1972 by Wilzbach and co-workers[29] for the conversion of *N*-methylpyridinium chloride to a bicyclic aziridine, photoirradiation of a pyridinium ion has been widely used with both functionalized pyridines and those containing a variety of *N*-alkyl substituents[30] for the synthesis of regiochemically and stereochemically substituted cyclopentanes.[31–33] Irradiation of *N*-allyl-pyridinium perchlorate salts without isolation of the aziridine intermediate prior to methanolysis has been reported.[34] Using a similar strategy, we prepared aziridine **22** through the *N*-allylpyridinium chloride **23**. The intermediate allylic cation, generated in the photochemical reaction is trapped by H_2O, reacting *trans* to the aziridine ring to yield **22** as a racemate in 60% yield (Scheme 2). Optimization of reaction conditions on a small scale (1 mmol) gave isolated yields ranging from 64 to 58%, depending on the counter-ion (X^- = Br^-, 64%; X^- = Cl^-, 60%;

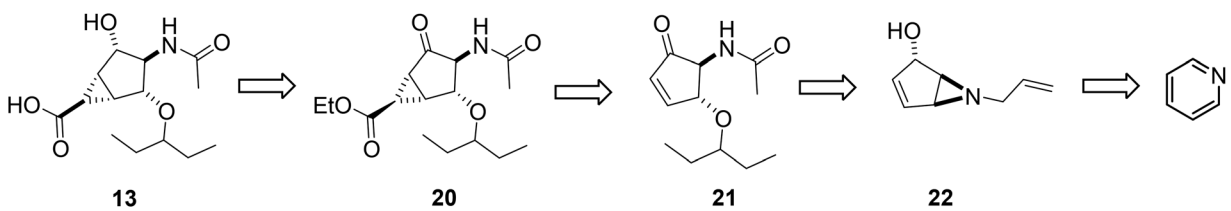

Scheme 1 Retrosynthetic analysis for compound **13**.

Open Access Article. Published on 07 June 2016. Downloaded on 11/1/2025 4:50:22 AM.
This article is licensed under a Creative Commons Attribution-NonCommercial 3.0 Unported Licence.

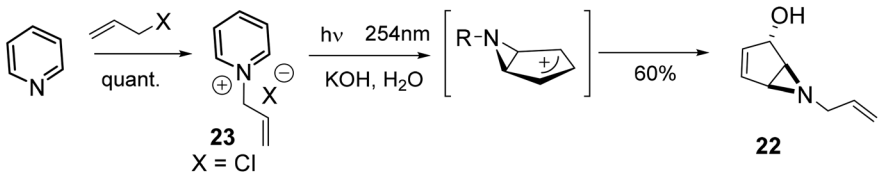

Scheme 2 *N*-Allylpyridinium salt photoirradiation.

$X^- = BF_4^-$, 58%). However, in general, scale-up to a 7–10 mmol scale produced lower yields (30–55%), due to the lability of the aziridine, although the reaction with *N*-allylpyridinium chloride **23** produced noticeably fewer impurities (55% isolated yield). Following benzoylation of **22** (95% yield), several conditions were examined for the opening of aziridine **24** by 3-pentanol (Scheme 3).[35–37]

The conditions reported by Trost and Zhang,[38] designed to generate strictly anhydrous conditions, with 3-pentanol as solvent and boron trifluoride etherate as the Lewis acid, however, only yielded compound **25** in 35% yield. Azeotropically drying the starting material **24** with toluene and using molecular sieves did not improve the conversion significantly, nor did the use of weaker Lewis acids such as copper triflate and trimethylsilyl triflate. We then observed that **25** formed more slowly but more efficiently at lower temperatures. That is, addition of substrate **24** (0.15 M) to boron trifluoride etherate in 3-pentanol at 0 °C, followed by overnight reaction at room temperature, resulted in the formation of **25** in 63% yield (Scheme 3). Removal of the *N*-allyl group from amine **25** was unsuccessful under a variety of standard conditions, including the use of Wilkinson's catalyst,[39] Pd/C in ethanolamine,[40] or $Pd(dba)_2$/DPPB (1 : 1) 5 mol% with 1.1 equivalent of 2-thiobenzoic acid.[41] We speculate that metal-catalyzed removal of the *N*-allyl group[42] most likely competes with the cross-reactivity of the cyclopentene double bond and this leads to decomposition of the substrate. Next, we tried to remove the *N*-allyl group using potassium *tert*-butoxide in DMSO.[43] However, in addition to removing the benzoate group, the *N*-allyl group remained intact even upon treatment with *t*-BuOK in DMSO at room temperature for 48 h or at 100 °C for 6 h. To circumvent this problem the acetamide **26** was prepared by acylation of **25** (Scheme 3). Again, neither Pd/C nor $Pd(OCOCF_3)_2$: DPPP 1 : 1 (10 mol%)[44] gave more than a 10% conversion to the desired enamine isomer **31** (Scheme 4).

Unexpectedly, cleavage of enamine **31** to give **32** occurred spontaneously in $CDCl_3$, as observed during ^{1}H-NMR analysis (Fig. S1†). Finally, treatment of **26** with potassium *tert*-butoxide in DMSO afforded the desired allylic isomerization along with removal of both the amide and the benzoate groups (Scheme 4) to give enamine **33**, which also cleaved in $CDCl_3$. Compound **27** was therefore obtained by the following procedure: **33** was converted to **34** by dissolving it in $CDCl_3$ and storing it at room temperature for 15 days, while monitoring the reaction by NMR spectroscopy (Fig. S2†). The reaction was

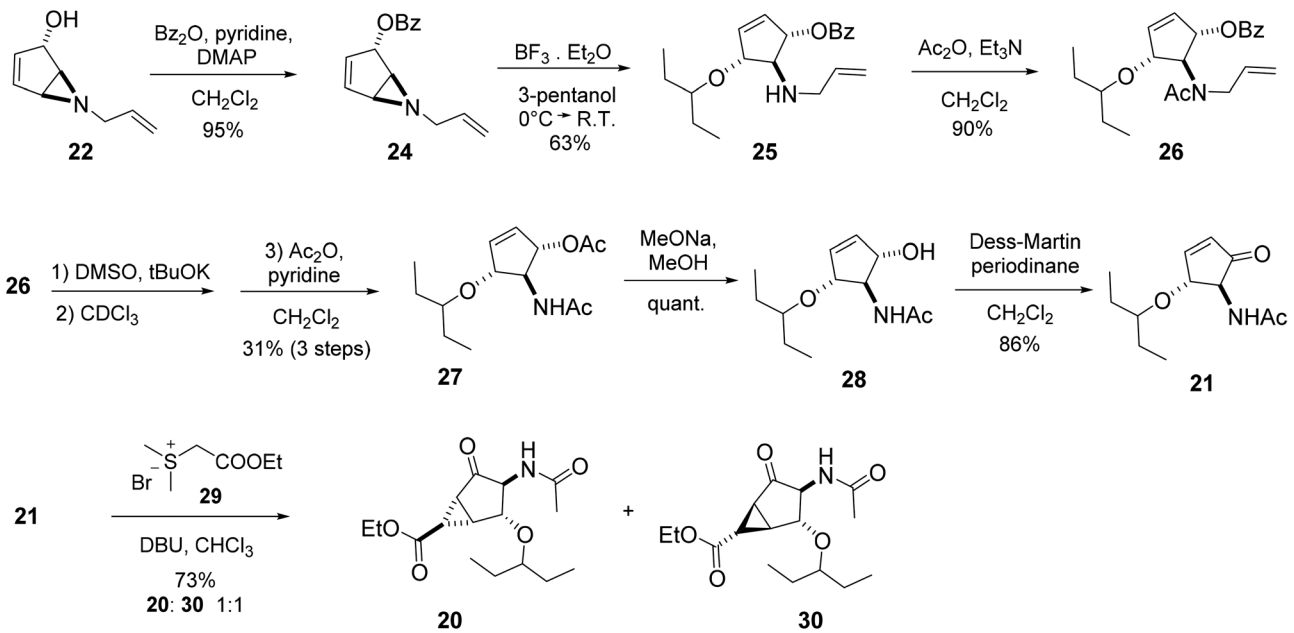

Scheme 3 Synthetic route to the intermediates **20** and **30**.

Open Access Article. Published on 07 June 2016. Downloaded on 11/1/2025 4:50:22 AM.
This article is licensed under a Creative Commons Attribution-NonCommercial 3.0 Unported Licence.

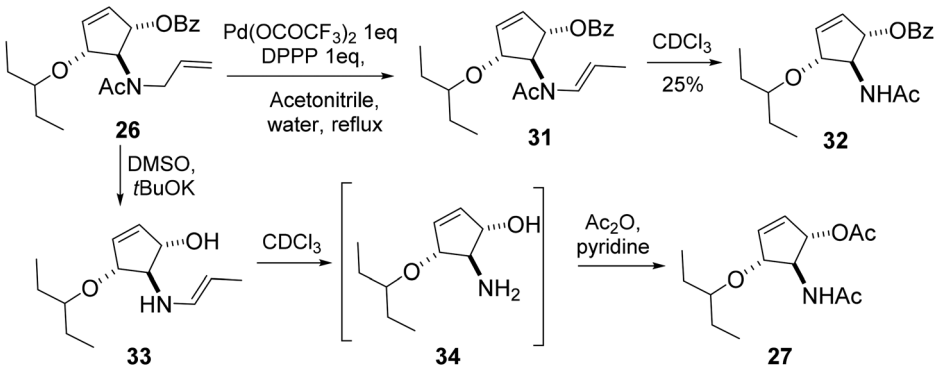

Scheme 4 *N*-Deallylation reaction: synthesis of **27**.

ascribed to solvent residual acidity and did not occur in $CHCl_3$. Extensive efforts were made to optimize the conditions using H_2SO_4 in either $CHCl_3$ or acetone, and HCl in MeOH. However, these reactions resulted in partial decomposition as well as rearrangement of the endocyclic double bond. Observations reveal the lability of the free amino hydroxyl derivative **34** under acidic conditions. Although not ideal, cleavage in deuterated chloroform represents a mild solution, avoiding product decomposition and endocyclic double bond isomerization.

As the amino alcohol **34** could not be isolated without extensive decomposition, it was directly acetylated (acetic anhydride, pyridine) to give **27** (31% yield from **26**). Direct cyclopropanation of **27** was attempted using ethyl diazoacetate with various rhodium and copper catalysts,[45] but without success. Thus, ketone **21** was prepared by *O*-deacetylation (MeONa, MeOH) and Dess–Martin oxidation (Scheme 3), and it was subjected to a Johnson–Corey–Chaykovsky cyclopropanation by addition of a nucleophilic sulfur ylide.[46] In particular, reaction of the unsaturated ketone **21** with the sulfonium ylide, formed *in situ* by treatment of the sulfonium salt **29** with DBU (1,8-diazobicyclo[5.4.0]undec-7-ene), gave the diastereomers **20** and **30** (1 : 1 ratio, Scheme 3), which were separated by flash chromatography. Stereochemical assignment for **20** and **30** was based on ^{1}H-NMR coupling constants and chemical shifts, values which matched those reported for substituted bicyclo[3.1.0]hexane derivatives (for a full discussion of assignments see the ESI and Fig. S3†).[47,48] Ketones **20** and **30** were then subjected to reduction with polymer-supported borohydride on Amberlite® to produce the corresponding alcohols (Scheme 5).

Reduction of **20** afforded **35** in 90% yield by preferential hydride attack from the top, less hindered face. In contrast, hydride addition to substrate **30** led to two diastereoisomers

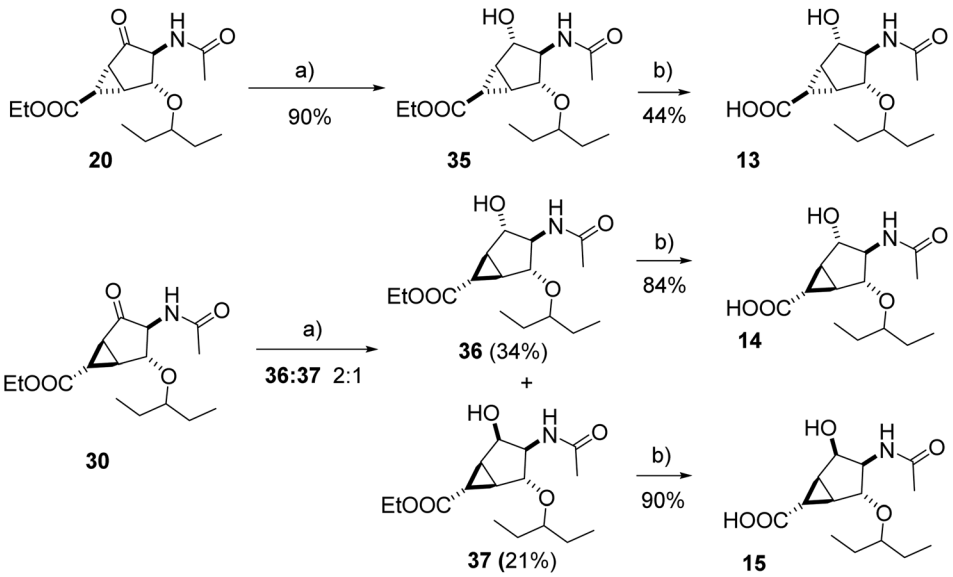

Scheme 5 Reduction of ketones **20** and **30** and ester hydrolysis. Reaction conditions: (a) polymer-supported borohydride, MeOH, r.t., 5 h. (b) NaOH, MeOH, water, 4 °C, overnight.

Open Access Article. Published on 07 June 2016. Downloaded on 11/1/2025 4:50:22 AM.
This article is licensed under a Creative Commons Attribution-NonCommercial 3.0 Unported Licence.

36 and **37** in ~2 : 1 ratio (^{1}H NMR), in 34% and 21% isolated yields, respectively.

Stereochemical assignments were confirmed by ^{1}H-NMR spectroscopy (Fig. 5) using typical coupling-constant data for bicyclo[3.1.0]hexane derivatives systems.[47,48] Compound **35** (Fig. 5, top panel) showed coupling constants consistent with two *cis* relationships (J_{1-2} = 6.6 Hz, J_{4-5} = 4.2 Hz). The coupling constant values for compound **36** (Fig. 5, middle panel) are in agreement with both *trans* relationships ($J_{1-2} = J_{4-5}$ = ~0 Hz). Compound **37** (Fig. 5, bottom panel) showed a *cis* H_1/H_2 relationship (J_{1-2} = 4.6 Hz) and no coupling constant for *trans* H_4/H_5. In addition, significant chemical shift differences were noted for protons shielded or deshielded by the cyclopropyl ring, especially H_2 and H_3 (Fig. 5).

Stereochemical assignments were verified through observation of NOE contacts between non-vicinal protons. A striking example is provided by the contact between H_6 on the cyclopropyl ring and H_2 and/or H_4 on the cyclopentyl ring, which showed strong contacts for a *cis* orientation (*e.g.* **36**) but only weak contacts for a *trans* orientation (*e.g.* **35**, **37**) (Fig. 6), consistent with literature data.[49]

Hydrolysis of the ethyl esters in **35–37** was accomplished with sodium hydroxide, in MeOH : H_2O 5 : 1 at 4 °C, to give compounds **13–15** (Scheme 5).

To synthesize amines **16** and **17** (Scheme 6), reductive amination of **20** with sodium triacetoxyborohydride and glacial AcOH in THF was used, following the procedure reported by Abdel-Magid *et al.*[50] A single isomer was generated, resulting from addition of hydride from the less hindered face, which led to the formation of the benzylamine derivative **16** and the 4-phenylbenzylamine derivative **17** in 59% and 60% yields, respectively, after ethyl ester removal under basic con-

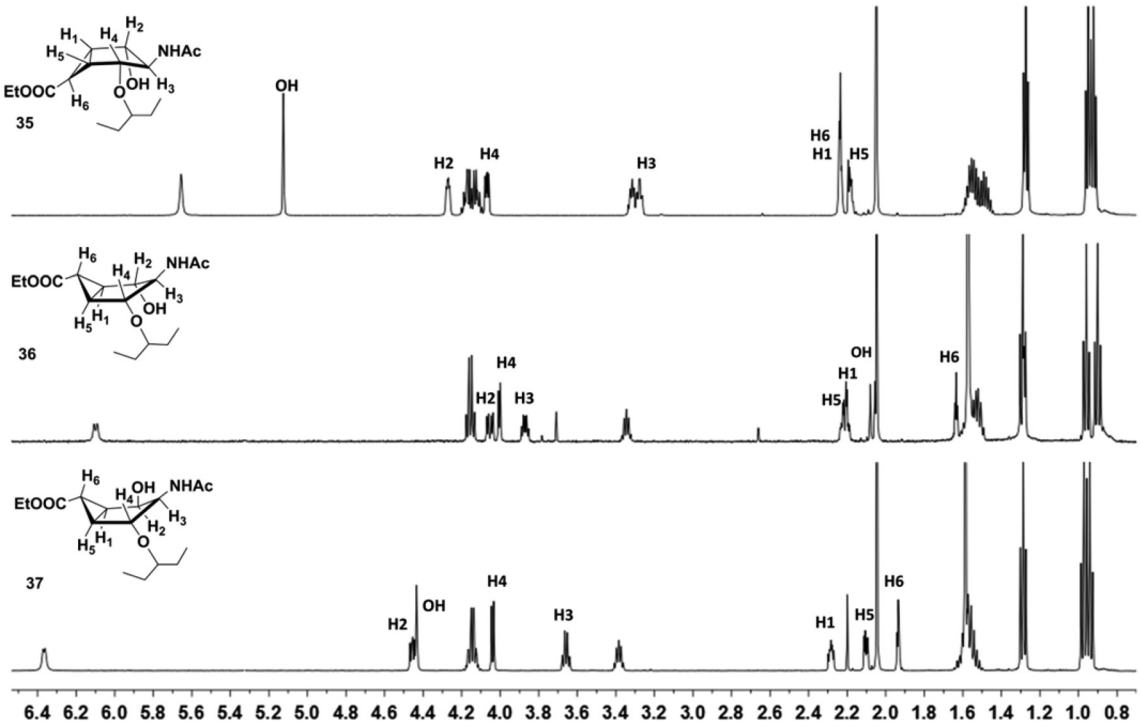

Fig. 5 ^{1}H-NMR spectra of compound **35** (top panel), **36** (middle panel), **37** (bottom panel). The proton spectral assignments are also shown for all compounds.

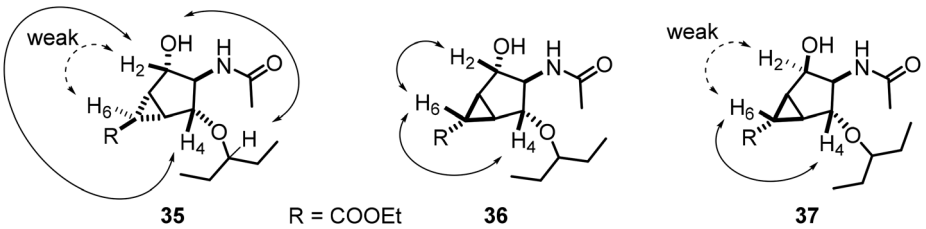

Fig. 6 NOEs of compounds **35**, **36**, **37**.

Open Access Article. Published on 07 June 2016. Downloaded on 11/1/2025 4:50:22 AM.
This article is licensed under a Creative Commons Attribution-NonCommercial 3.0 Unported Licence.

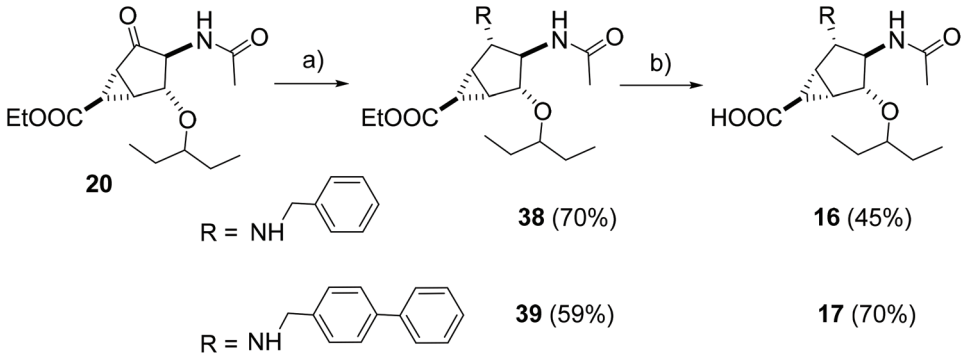

Scheme 6 Reductive amination of **20** and ester hydrolysis of **38** and **39**. Reaction conditions: (a) $Na(CH_3COO)_3BH$, AcOH, dry THF, amine, 8 h (b) NaOH, MeOH, water, 4 °C, overnight.

ditions (Scheme 6). Attempts to perform reductive amination with derivative **30** gave a complex mixture of products.

Enzyme inhibition

We note that all compounds made by us are racemates, as a result we expect that the IC_{50} values for the enantiomer that resembles D-sialic acid will be one half of that measured. Nevertheless, we report the measured values for the racemic mixtures. Of note, compounds **13**, **16**, and **17** share the stereochemical features of α-sialic acid, while compounds **14** and **15** (epi-C4) possess the stereochemistry associated with β-sialic acid.

Compounds **13–17** were each evaluated using an enzyme inhibitory assay that involves measuring the hydrolysis of the fluorogenic substrate 2-(4-methylumbelliferyl) α-D-acetylneuraminide sodium salt hydrate (MUNANA) over a period of time to check for "slow-binding" inhibition. As a result, such inhibition assays often involve a preincubation step of the inhibitor with the enzyme prior to substrate addition, which initiates the enzymatic reaction that is monitored by measuring the fluorescence of the cleaved substrate. The use of different protocols with different preincubation times (as well as buffer, pH and temperatures) can affect the IC_{50} values and has resulted in a plethora of literature values, which makes valid comparisons difficult to achieve. Indeed, it is now well known that influenza neuraminidase inhibitors zanamivir, oseltamivir and peramivir are "slow-binding" inhibitors that show a slow equilibrium formation of a tight inhibitor–enzyme complex.[51] Specifically, if the enzymatic reaction is initiated before equilibrium has been established, the resulting activity data will not yield accurate K_i values. A real-time kinetic assay recently reported by Barrett *et al.*[52] has been shown to be suitable for the evaluation of time-dependent changes in IC_{50} values, and thus we used this method for the measurement of compound activity as well as to determine if our compounds show "slow-binding" kinetics. All compounds were tested as inhibitors against two neuraminidases from influenza type A, one representing group-1 (H5N1) and one group-2 (H9N2). Compound **4** (Fig. 1), a known nanomolar inhibitor of influenza A neuraminidase[10] (K_i = 0.46 nM; H5N1), was used as a positive control in this real-time assay. IC_{50} values were calculated for consecutive 10 min intervals, using a range of concentrations, for each inhibitor over a period of 60 minutes.

First, the data show that the enzymatic activity changes significantly during the experimental time course for all of our compounds, including **4** (Table 1, initial slope and final slope columns) with both enzymes. An example of this behaviour is shown in Fig. 7 (left panel) for the inhibition of the H9N2 neuraminidase by compound **16**, which clearly shows non-linear enzyme activity *versus* time.

In contrast, when the same experiment is performed after a 45 min preincubation of inhibitor **16** and protein, a linear response is obtained (Fig. 7, right panel; see ESI† for kinetics observed with the other compounds). Therefore, IC_{50} values were calculated from the measurements made after the neuraminidase and each inhibitor had been pre-incubated together for 45 minutes before addition of substrate. These values are listed in Table 1 (incubation column).[6,51–53] Of note, the IC_{50} values obtained after preincubation of **13–17** (Table 1) are uniformly lower than those measured for reactions without preincubation. Our measured value of 0.78 nM (IC_{50}) for **4** with the H5N1 enzyme is consistent with the literature K_i value,[10] which justifies the use of the current kinetic protocols.

Second, alcohols **13** and **14** inhibit both enzymes with similar IC_{50} values that are around 20–60 μM, whereas the C4-epimer (**15**) is totally inactive. A comparison between **13** and **14** shows that the β-sialic acid mimic **14** binds tighter to the enzyme active sites. A similar observation was reported for the phosphonate inhibitor ePANA **18**, which binds more tightly relative to aPANA **19** (Fig. 3).[28] This observation is consistent with that made by Newstead *et al.* for nucleophilic mutant neuraminidases where the chair form of β-sialic acid binds preferentially,[54] a result of lower steric strain. Whereas, in native neuraminidases only the α-sialic acid can bind, albeit in a boat conformation.

Third, replacing the hydroxyl group of **13** with *p*-phenylbenzyl amine in **17** led to tighter binding to the N2 (IC_{50} = 11 μM) and N1 (IC_{50} = 10 μM) enzymes. Unfortunately, with the synthetic approaches used so far we could not access the amines corresponding to framework **14**. The slight improvement of **17** may conceivably arise from replacement of the hydroxyl group

Open Access Article. Published on 07 June 2016. Downloaded on 11/1/2025 4:50:22 AM.
This article is licensed under a Creative Commons Attribution-NonCommercial 3.0 Unported Licence.

Table 1 IC_{50} values calculated from the real-time kinetic experiments. The values were obtained as relative slope of each time interval[a] *versus* total fluorescent units (FU) for A/Chicken/HongKong/G9/1997 H9N2 and A/Anhui/1/2005 H5N1[b]

	N2			N1		
Compound	IC_{50} (μM) initial slope[c]	IC_{50} (μM) final slope[c]	IC_{50} (μM) incubation[d]	IC_{50} (μM) initial slope[c]	IC_{50} (μM) final slope[c]	IC_{50} (μM) incubation[d]
13	717	105	40	452	65	64
14	453	35	23	813	188	48
15	1080	n.d.	329	840	452	n.d.
16	591 (0–5 min)[e] 208 (5–10 min)[e]	33	23	2895	151	49
17	388 (0–3 min)[e] 215 (3–10 min)[e]	22	11	661	53	10
4[f]	0.05	5.7×10^{-4}	4.5×10^{-4}	0.108	1.65×10^{-3}	7.8×10^{-4}

[a] Initial slope refers to the first time interval of constant slope (0–10 min or 0–5 min generally, depending on the inhibitor curves). The interval is fixed for each series of concentrations for that specific inhibitor. Final slope refers to the last time interval of constant slope (50–60 min generally). Values represent the average of duplicate experiments. The standard deviations were all <15%. [b] Rates in FU min^{-1} were calculated for each concentration and for each time interval. The IC_{50} value is the inhibitor concentration that inhibits the rate of the uninhibited control by 50%. This approach separates each reaction time so it is independent of the rates of preceding time intervals. [c] No preincubation. [d] Preincubation with inhibitor for 45 min. [e] Values reported to underline a significant variation of slope during the first minutes of analysis, affecting the relative IC_{50} values. [f] Compound **4** (Fig. 1) was used as positive control.

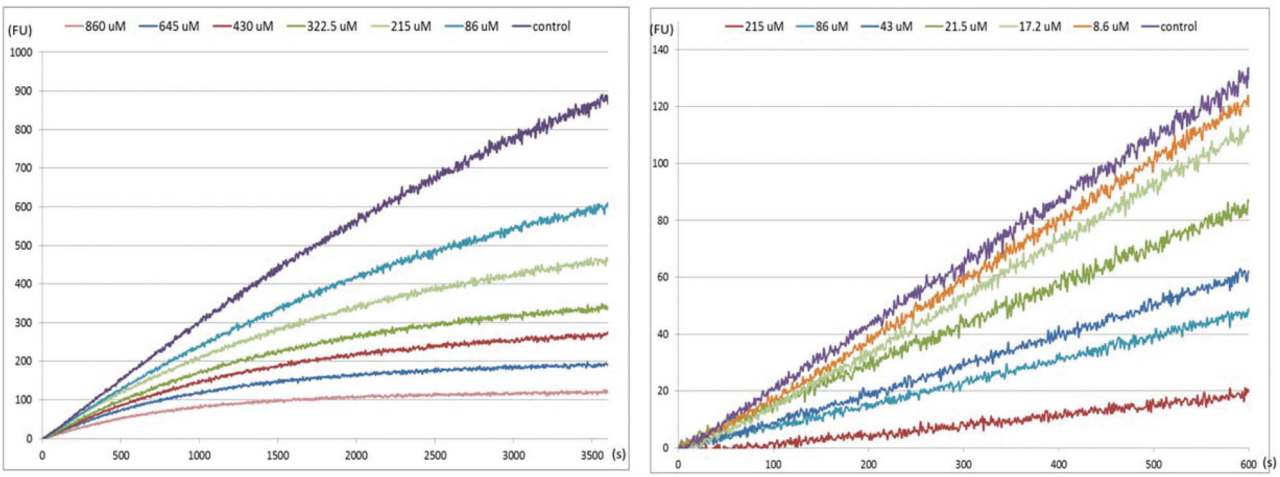

Fig. 7 Comparison of preincubation or no preincubation curves with inhibitor **16** on the enzyme activity of A/Chicken/HongKong/G9/1997 H9N2 (left panel: no preincubation, 0–60 min acquisition. Right panel: 45 min preincubation, 0–10 min acquisition).

of **13** with a basic nitrogen and/or additional interactions of the lipophilic group within the 150-cavity. It is well known that replacement of the natural C-4 OH group on the sialic acid glycal framework by either an amino or guanidino (zanamivir, **2**) group enhances binding by factors of 100 and 500, respectively.[25] The minor change of activity on going from **13** to **17** clearly indicates that interaction of the current inhibitors with the neuraminidase active site still needs to be optimized. Also, there is no reason to suppose that the optimal ether side chain for the bicyclo[3.1.0]hexyl system will be the 3-pentyl group, which was originally optimized on the cyclohexene framework of oseltamivir (**1**).[2] Indeed, it is known that **4** is less active than zanamivir **2**,[10] most likely because the cyclohexene framework of **4** does not optimally place the 3-pentyl side chain and the guanidino group within the neuraminidase active site. Clearly, given that all of our bicyclo[3.1.0]hexane inhibitors were at least four orders of magnitude less active than the control, this rigid carbon skeleton does not produce the same set of interactions as the cyclohexene or glycal frameworks used so far. However, it is noticeable that the locked boat-like conformation of the [3.1.0] fused system is showing a viable novel framework for neuraminidase inhibition. Further studies are currently underway to understand this aspect and improve interactions with future inhibitors.

Last, it is interesting that all the bicyclic inhibitors displayed the hallmark signs of "slow binding" inhibition. In general, key factors related to time-dependent binding kinetics have been proposed to be due to ligand exchange, hydrogen-bond rearrangement and the local-conformation change of the receptor to accommodate the ligand toward formation of the Michaelis complex, which would take the so-called "target-resident time" to reach the optimal binding mode.[6,52] For

 This journal is © The Royal Society of Chemistry 2016

Open Access Article. Published on 07 June 2016. Downloaded on 11/1/2025 4:50:22 AM.
This article is licensed under a Creative Commons Attribution-NonCommercial 3.0 Unported Licence.

instance, the slow binding mode of zanamivir **2** has been rationalized by the observation that a water molecule must be displaced before the guanidinium group can bind tightly in the active site.[51] That can also explain the slow binding behavior of compound **4** (Table 1). In contrast, slow-binding of oseltamivir has been ascribed to the mandatory side chain rotation of E276 (N2 numbering) in the neuraminidase active site to accommodate the 3-pentyl ether side chain.[53] We note that observation of time-dependent changes or so-called 'slow binding' competitive inhibition generally arises from one of two main sources, (i) a low concentration of inhibitor used to determine its IC_{50}; or (ii) a slow conformational change in the enzyme from a weak binding to a tight binding complex.[55] In the current case, we attribute the changes in IC_{50} values to a slow conformational change, because the inhibitor IC_{50} values of compounds **13–17** are in the low micromolar range.

Conclusion

In conclusion, we have successfully synthesized constrained oseltamivir analogues, based on a bicyclo[3.1.0]hexane scaffold using a photochemical reaction and a Johnson–Corey–Chaykovsky cyclopropanation. These new candidate inhibitors were designed to target the catalytic site and possibly to mimic a distorted boat conformation that occurs during transformation of the Michaelis complex to the glycosyl-enzyme intermediate with the goal of mimicking the glycosylation transition state structure. Two of the compounds, analogues of α- and β-sialic acid, showed promising inhibitory activity against N1 and N2 viral neuraminidases and the kinetic analyses showed 'slow-binding', time-dependent inhibition. Two amino derivatives were also synthesized with the aim of occupying the adjacent 150-cavity. In particular, the 4-phenylbenzyl derivative displayed an increased binding affinity. These results provide insight into the requirements for the configuration of constrained cyclopropyl sialic analogues and lay the groundwork for further development of novel constrained inhibitors that are effective against influenza A neuraminidases through additional cavity occupation.

Experimental

General information

All chemicals were of analytical grade or better and were purchased from Sigma-Aldrich unless noted otherwise. ^{1}H- and ^{13}C-NMR spectra were acquired on a Bruker instrument and recorded at 600 or 400 MHz and 150 or 100 MHz, respectively. Spectra are reported as follows: chemical shift (δ ppm), multiplicity (s = singlet, d = doublet, t = triplet, q = quartet, quint = quintet, m = multiplet, bs = broad singlet), coupling constants (Hz). All assignments were confirmed with the aid of two-dimensional ^{1}H–^{1}H (COSY), ^{1}H–^{13}C (HSQC) and/or ^{1}H–^{13}C (HMBC) experiments using standard pulse programs. Processing of the spectra was performed using MestReNova software. Product numbering for spectral assignment is reported in the ESI† and is shown in Fig. 5. Analytical thin-layer chromatography (TLC) was performed on aluminum plates pre-coated with silica gel 60F-254. The developed plates were air dried, exposed to UV light, and/or sprayed with a solution containing molybdic reagents or permanganate reagents, and heated. Column chromatography was performed with an automated flash chromatography system. High resolution mass spectra were obtained by the electrospray ionization method, using a TOF LC/MS high-resolution magnetic sector mass spectrometer. Preparative photochemical reactions were conducted using a Rayonet photochemical chamber reactor (RPR-100) and a bank of 254 nm lamps. The photolysis solutions were purged with N_2 both before and during irradiation. The progress of preparative photochemical reactions was monitored by ^{1}H NMR spectroscopy.

NA enzyme inhibitory assay

A/Chicken/HongKong/G9/1997 H9N2 and A/Anhui/1/2005 H5N1 were purchased from SinoBiochemical. The NA inhibition assay was performed according to a standard method,[56] with minor modification as reported by Barrett *et al.*[52] Accordingly, the substrate 2-(4-methylumbelliferyl) α-D-acetylneuraminic acid sodium salt hydrate (MUNANA; Sigma M8639) is cleaved by the enzyme to yield a quantifiable fluorescent product, measured during the assay. The fluorescence was assessed using an excitation wavelength of 365 nm and an emission wavelength of 450 nm and substrate blanks were subtracted from the sample readings. Stock solutions of influenza viruses (H5N1 and H9N2) were freshly prepared by dissolution in MES buffer (32.5 mM 2-(*N*-morpholino)ethanesulfonic acid, 4 mM $CaCl_2$, pH 6.5) at a concentration of 10 U mL^{-1}. Enzyme activity was titrated for both viruses to ensure linearity of the enzymatic reaction over time. Inhibitors were dissolved in DMSO at 20 mM initial concentration. Dilutions of inhibitors were performed in MES buffer, ranging from 1 mM to 1 μM and 5–7 serial dilutions were used; the concentrations depended on the appropriate range for IC_{50} determination, identified for each inhibitor.

No preincubation assay

86 μL of inhibitor solution, 2 μL of 0.2 M of $CaCl_2$, and 2 μL of 10 mM MUNANA were incubated for 5 min at 37 °C. Then 10 μL of stock solution was added to start the reaction. Fluorescence was measured for 60 min after the addition of enzyme, and linear slopes were determined for each consecutive 10 minute time interval. Graphs of $\log_{10}$ concentration of inhibitor *versus* percent enzyme inhibition compared to the control were plotted after 10, 20, 30, 40, 50 and 60 min, to calculate IC_{50} for each interval. The IC_{50} is the ligand concentration leading to 50% inhibition of the rate of the reaction, compared to the control rate with no inhibitor, calculated using a nonlinear regression function in GraphPad Prism.

Preincubation assay

86 μL of inhibitor solution and 10 μL of neuraminidase stock solution were preincubated for 45 min at 37 °C, in the

Open Access Article. Published on 07 June 2016. Downloaded on 11/1/2025 4:50:22 AM.
This article is licensed under a Creative Commons Attribution-NonCommercial 3.0 Unported Licence.

presence of $CaCl_2$. The reaction was initiated by the addition of the substrate (MUNANA) and fluorescence was measured for 10 min.

***N*-Allyl-pyridinium chloride (23).** Allyl chloride (1.9 mL, 23.38 mmol, 1 equiv.) was added to pyridine (2.5 mL, 30.39 mmol, 1.3 equiv.) under N_2 and the reaction was stirred at 90 °C for 4 h. Evaporation of the solvent and coevaporation with toluene and CH_2Cl_2 yielded compound **23** as a light-brown solid (3.6 g, 98%). The analytical data were consistent with those reported in the literature.[34] ^{1}H NMR (400 MHz, D_2O) δ 8.86 (d, J = 6.2 Hz, 2H), 8.58 (t, J = 7.8 Hz, 1H), 8.09 (t, J = 6.7 Hz, 2H), 6.27–6.06 (m, 1H), 5.57 (d, J = 10.3 Hz, 1H), 5.49 (d, J = 17.1 Hz, 1H), 5.24 (d, J = 6.2 Hz, 2H).

Compound 22. *N*-Allylpyridinium chloride **23** (1.190 g, 7.65 mmol, 1 equiv.) was dissolved in water (850 mL) in a quartz vessel and KOH (430 mg, 7.65 mmol, 1 equiv.) was added. The reaction mixture was purged with nitrogen bubbling for 1 h. The solution was irradiated with 15 mercury lamps (8 W each) for 16 h, under nitrogen bubbling and stirring (nitrogen bubbling during the reaction course was necessary to prevent side reactions). Complete starting material consumption (disappearance of aromatic protons) was monitored by ^{1}H-NMR. Reactions were performed on a maximum scale of 10 mmol. The solvent was removed under reduced pressure to obtain a dark yellow solid, which was triturated with $CHCl_3$: acetone 1 : 1 and filtered. The organic phase was evaporated and the yellow oil obtained was then purified over basic alumina (R_f = 0.37; 6 : 4 acetone : $CHCl_3$, $KMnO_4$ stain) to afford compound **22** as an oil (630 mg, 60% yield). ^{1}H NMR (400 MHz, $CDCl_3$) δ 6.26 (dd, J_{1-5} = 5.6 Hz, J_{1-3} = 0.8 Hz, 1H, H_1), 5.95–5.80 (m, 2H, H_5, H_7), 5.18 (dd, $J_{8a-7trans}$ = 17.2, J_{6-8a} = 1.6 Hz, 1H, H_{8a}), 5.11 (dd, $J_{8b-7cis}$ = 10.4, J_{6-8b} = 1.6 Hz, 1H, H_{8b}), 4.47 (bs, 1H, H_2), 2.96 (dd, J_{6a-6b} = 14.1, J_{6a-7} = 5.7 Hz, 1H, H_{6a}), 2.88 (dd, J = 14.1, J_{6b-7} = 5.7 Hz, 1H, H_{6b}), 2.54 (m, 2H, H_4, OH), 2.48 (dd, J_{3-4} = 4.3 Hz, J_{3-5} = 1.7 Hz, 1H, H_3). ^{13}C NMR (100 MHz, $CDCl_3$) δ 137.56 (C_1), 135.52 (C_5), 134.64 (C_7), 116.78 (C_8), 74.95 (C_2), 60.22 (C_6), 50.50 (C_3), 46.78 (C_4). HRMS: (ESI) m/z calculated for $[C_8H_{12}NO]^+$ 138.09123; found 138.09134.

Compound 24. To a stirred solution of compound **22** (1.88 g, 13.7 mmol, 1 equiv.) in dry CH_2Cl_2 (1 mL), pyridine (2.77 mL, 34.2 mmol, 2.5 equiv.) and benzoic anhydride (3.72 g, 16.4 mmol, 1.2 equiv.) were added under nitrogen atmosphere. 4-Dimethylaminopyridine (DMAP) (0.33 g, 2.7 mmol, 0.2 equiv.) was added and the resulting mixture was stirred for 4 h at room temperature (TLC 6 : 4 acetone : $CHCl_3$, R_f = 0.92, $KMnO_4$ stain). The reaction mixture was diluted with CH_2Cl_2 and washed with 0.1 M $NaHSO_4$ and saturated $NaHCO_3$, (three times each alternating acid and basic wash), then with saturated NaCl. The organic phase was then dried with sodium sulfate. The solvent was evaporated and the crude material was filtered on basic alumina, eluting with $CHCl_3$ to afford **24** (3.13 g; 95% yield). ^{1}H NMR (500 MHz, $CDCl_3$) δ 8.03 (d, J = 7.9 Hz, 2H, Ar-H), 7.53 (t, J = 7.4 Hz, 1H, Ar-H), 7.41 (t, J = 7.7 Hz, 2H, Ar-H), 6.42 (d, J_{1-5} = 5.6 Hz, 1H, H_1), 5.91 (m, 2H, H_5, H_7), 5.69 (s, 1H, H_2), 5.23 (dd, $J_{8-7trans}$ = 17.2 Hz, J_{6-8a} = 1.4 Hz, 1H, H_{8a}), 5.14 (d, J_{8-7cis} = 10.4 Hz, 1H, H_{8b}), 2.98 (d, J_{6-7} = 5.5 Hz, 1H, H_6), 2.70–2.67 (m, 1H, H_4), 2.64 (m, 1H, H_3). ^{13}C NMR (125 MHz, $CDCl_3$) δ 165.81 (CO), 138.02 (C_1), 134.49 (C_7), 133.86 (C_5), 133.13 (C_{Ar}), 129.72 (C_{Ar}), 128.40 (C_{Ar}), 116.80 (C_8), 77.24 (C_2), 60.20 (C_6), 47.79 (C_3), 46.84 (C_4). HRMS: (ESI) m/z calculated for $[C_{15}H_{16}NO_2]^+$ 242.11789; found 242.11755.

Compound 25. Compound **24** (1.45 g, 6 mmol, 1 equiv.) was dissolved in 3-pentanol (40 mL) under nitrogen atmosphere. $BF_3{\cdot}Et_2O$ (0.80 mL, 6.05 mmol, 1.08 equiv.) was added at 0 °C under stirring and the solution turned blue. The solution was stirred overnight at room temperature. The reaction mixture was diluted with CH_2Cl_2 (80 mL) and basic alumina was added (300 g) and stirred vigorously. The slurry was then loaded on a column and eluted with 1 : 1 $CHCl_3$: acetone to obtain compound **25** (1.24 g; 63% yield). ^{1}H NMR (500 MHz, $CDCl_3$) δ 8.05 (d, J = 7.3 Hz, 2H, Ar-H), 7.56 (t, J = 7.4 Hz, 1H, Ar-H), 7.44 (t, J = 7.7 Hz, 2H, Ar-H), 6.07 (d, J_{1-5} = 5.9 Hz, 1H, H_1), 5.98–5.87 (m, 2H, H_5, H_7), 5.55 (bs, 1H, H_2), 5.20 (d, $J_{8-7trans}$ = 17.2 Hz, 1H, H_{8a}), 5.09 (d, J_{8-7cis} = 10.4 Hz, 1H, H_{8b}), 4.26 (m, 1H, H_4), 3.44 (t, J_{2-3} = J_{3-4} = 3.9 Hz, 1H, H_3), 3.41–3.31 (m, 2H, H_9, H_6), 1.55 (quint, J_{10-11} = 7.3 Hz, 4H, H_{10}), 0.93 (td, J_{10-11} = 7.3, 4.4 Hz, 6H, H_{11}). ^{13}C NMR (125 MHz, $CDCl_3$) δ 166.68 (CO), 136.56 (C_7), 135.98 (C_1), 133.21 (C_{Ar}), 130.88 (C_5), 130.19 (C_{Ar}), 129.86 (C_{Ar}), 128.50 (C_{Ar}), 116.24 (C_8), 86.47 (C_4), 83.33 (C_2), 81.74 (C_9), 71.62 (C_3), 50.96 (C_6), 26.62 (C_{10}), 26.47 (C_{10}), 10.00 (C_{11}), 9.62 (C_{11}). HRMS: (ESI) m/z calculated for $[C_{20}H_{28}NO_3]^+$ 330.20636; found 330.20637. m/z calculated for $[C_{20}H_{27}NNaO_3]^+$ 352.18802; found 352.18831.

Compound 26. To a stirred solution of compound **25** (760 mg, 2.3 mmol, 1 equiv.) in dry CH_2Cl_2 (15 mL), Et_3N (0.65 mL, 4.6 mmol, 2 equiv.) and 0.1 M acetic anhydride in CH_2Cl_2 (1.5 mL) were added under nitrogen atmosphere. The reaction mixture was stirred overnight at room temperature (TLC 8 : 2 Hex : EtOAc R_f = 0.36, UV and KMnO4 stain). The reaction mixture was diluted with CH_2Cl_2 and washed with 0.1 M $NaHSO_4$, saturated $NaHCO_3$ and with saturated NaCl. The organic phase was dried with sodium sulfate. The solvent was evaporated and the crude material was purified by flash chromatography (from 95 : 5 Hex : EtOAc to 8 : 2 Hex : EtOAc) to afford **26** (769 mg; 90% yield) (1 : 0.45 mixture of isomers around the amide bond A and B). ^{1}H NMR (600 MHz, $CDCl_3$) δ 8.06–7.94 (m, 4H, Ar-H), 7.61–7.51 (m, 2H, Ar-H), 7.48–7.39 (m, 4H, Ar-H), 6.23 (d, J_{2A-3A} = 5.1 Hz, 1H, H_{2A}), 6.11–6.06 (m, 2H, H_{1A}, H_{1B}), 6.02 (d, J_{1B-5B} = 6.2 Hz, 1H, H_{5B}), 5.98 (d, J_{1A-5A} = 6.1 Hz, 1H, H_{5A}), 5.96–5.89 (m, 1H, H_{7B}), 5.85–5.73 (m, 1H, H_{7A}), 5.19 (d, $J_{8-7trans}$ = 17.3 Hz, 1H, H_{8A}), 5.18–5.09 (m, 2H, H_{8B}), 5.07 (d, J_{8-7cis} = 10.3 Hz, 1H, H_{8A}), 4.90 (d, J_{3A-4A} = 4.9 Hz, 1H, H_{4A}), 4.55 (t, J_{3B-4B} = 5.9 Hz, 1H, H_{3B}), 4.48 (d, J = 5.9 Hz, 1H, H_{4B}), 4.09–3.98 (m, 2H, H_{6A}, H_{6B}), 3.93 (dd, J_{6-6} = 17.0, J_{6-7} = 6.2 Hz, 2H, H_{6A}, H_{6B}), 3.78 (t, J = 5.1 Hz, 1H, H_{3A}), 3.29 (dt, J = 11.8, 5.8 Hz, 2H, H_{9A}, H_{9B}), 2.28 (s, 3H, H_{AcB}), 2.13 (s, 3H, H_{AcA}), 1.58–1.45 (m, 4H, H_{10A}, H_{10B}), 0.90 (dt, J = 13.7 Hz, J = 7.5 Hz, 12H, H_{11A}, H_{11B}). ^{13}C NMR (150 MHz, $CDCl_3$) δ 171.48 (CO_{AcA}), 171.25 (CO_{AcB}), 166.32 (CO_{BzA}), 166.19 (CO_{BzB}), 135.85 (C_{1A}), 134.17 (C_{7B}), 133.57 (C_{7A}), 133.52 (C_{ArB}), 133.08 (C_{ArA}), 131.09 (C_{1B}), 130.95 (C_{5A}, C_{5B}), 130.34 (C_{ArA}),

Open Access Article. Published on 07 June 2016. Downloaded on 11/1/2025 4:50:22 AM.
This article is licensed under a Creative Commons Attribution-NonCommercial 3.0 Unported Licence.

129.81 (C_{ArB}), 129.77 (C_{Ar}), 129.74 (C_{Ar}), 129.65 (C_{ArA}), 128.67 (C_{ArB}), 128.55 (C_{ArB}), 128.45 (C_{ArA}), 117.64 (C_{8A}), 116.34 (C_{8B}), 82.78 (C_{9B}), 82.51 (C_{4A}), 82.23 (C_{9A}), 81.17 (C_{4B}), 79.03 (C_{2A}), 77.77 (C_{2B}), 73.92 (C_{3A}), 71.98 (C_{3B}), 54.69 (C_{6A}), 46.14 (C_{6B}), 26.57 (C_{10A}), 26.49 (C_{10A}), 26.44 (C_{10B}), 26.37 (C_{10B}), 22.75 (C_{AcA}), 22.18 (C_{AcB}), 9.86 (C_{11A}), 9.74 (C_{11B}), 9.64 (C_{11A}), 9.50 (C_{11B}). HRMS: (ESI) *m/z* calculated for $[C_{22}H_{30}NO_4]^+$ 372.21630; found 372.21629. *m/z* calculated for $[C_{22}H_{29}NNaO_3]^+$ 394.19852; found 394.19887.

Compound 27. Compound **26** (800 mg, 2.5 mmol, 1 equiv.) was dissolved in DMSO (12 mL). *t*BuOK (704 mg, 6.27 mmol, 2.9 equiv.) was added and the reaction mixture was stirred for 24 h at room temperature, then diluted with DMSO (12 mL) and stirred for an additional 24 h. The reaction mixture was diluted with water (40 mL) and extracted with $CHCl_3$ (50 mL seven times). The organic phase was then dried with sodium sulfate. The solvent was evaporated to dryness to remove DMSO completely. The crude material was dissolved in $CDCl_3$ (300 mL) and stored for 15 days at room temperature. Conversion from compound **33** to compound **34** was verified by ^{1}H NMR (see ESI†) and TLC (4 : 6 Hex : EtOAc compound **34** R_f = 0.12, $KMnO_4$ stain). Compound **33** ^{1}H NMR (400 MHz, $CDCl_3$) δ 6.12 (dq, J_{6-7} = 7.7 Hz, J_{6-8} = 1.7 Hz, 1H, H_6), 5.90 (s, 2H, H_1, H_5), 5.76–5.65 (m, 1H, H_7), 4.66–4.55 (m, 2H, H_4, H_2), 4.25 (t, J_{1-5} = 5.8 Hz, 1H, H_5), 3.32–3.16 (m, 1H, H_9), 1.69 (dd, J_{8-8} = 7.0 Hz, 1.7 Hz, 3H, H_8), 1.58–1.39 (m, 4H, H_{10}), 0.88 (t, J_{10-11} = 7.4 Hz, 6H, H_{11}). Compound **34** ^{1}H NMR (400 MHz, $CDCl_3$) δ 5.98–5.90 (m, 2H, H_1, H_5), 4.57 (bs, 2H, NH_2), 4.54 (d, J_{3-4} = 5.1 Hz, 1H, H_4), 4.37 (d, J_{2-3} = 6.4 Hz, 1H, H_2), 3.88–3.73 (m, 1H, H_3), 3.33 (quint, J_{9-10} = 6.0 Hz, 1H, H_9), 1.68–1.43 (m, 4H, H_{10}), 1.00–0.86 (m, 6H, H_{11}). ^{13}C NMR (150 MHz, $CDCl_3$) δ 172.63 (CO_{Ac}), 134.37 (C_5), 131.85 (C_1), 84.43 (C_4), 81.29 (C_9), 79.62 (C_2), 68.92 (C_3), 26.83 (C_{10}), 26.69 (C_{10}), 9.84 (C_{11}), 9.80 (C_{11}). Compound **34** was not isolated due to its instability, the reaction mixture was concentrated to 10 mL, then 6 mL of $CHCl_3$ was added to a final concentration of 0.15 M. Pyridine (0.65 mL, 8 mmol, 3.2 equiv.) and acetic anhydride (0.71 mL, 7.5 mmol, 3 equiv.) were added under nitrogen atmosphere. 4-Dimethylaminopyridine (DMAP) (61 mg, 0.44 mmol, 0.2 equiv.) was added and the resulting mixture was stirred for 8 h at room temperature (TLC 4 : 6 Hex : EtOAc R_f = 0.28, $KMnO_4$ stain). The solvent was evaporated and the crude material was purified by flash chromatography (from 7 : 3 Hex : EtOAc to 0 : 100 Hex : EtOAc in 15 CV (column volume)) to afford **27** (466 mg; 80% yield) (based on compound **26**). Compound **27** ^{1}H NMR (500 MHz, $CDCl_3$) δ 6.12 (d, $J_{3\text{-}NH}$ = 7.8 Hz, 1H, NH), 6.01 (d, J_{1-5} = 6.0 Hz, 1H, H_5), 5.85 (d, J = 6.0 Hz, 1H, H_1), 5.55 (d, J_{2-3} = 4.3 Hz, 1H, H_2), 4.48 (d, J_{3-4} = 4.2 Hz, 1H, H_4), 3.98–3.93 (m, 1H, H_3), 3.34 (quint, J_{9-10} = 5.8 Hz, 1H, H_9), 2.03 (s, 3H, CH_{3NHAc}), 1.97 (s, 3H, CH_{3OAc}), 1.52–1.42 (m, 4H, H_{10}), 0.88 (dt, J = 12.1 Hz, J_{10-11} = 7.4 Hz, 6H, H_{11}). ^{13}C NMR (125 MHz, $CDCl_3$) δ 171.00 (CO_{NHAc}), 170.39 (CO_{Ac}), 136.09 (C_5), 130.89 (C_1), 83.98 (C_4), 81.93 (C_9), 80.43 (C_2), 63.89 (C_3), 26.67 (C_{10}), 26.37 (C_{10}), 23.46 (C_{NHAc}), 21.17 (C_{Ac}), 9.85 (C_{11}), 9.54 (C_{11}). HRMS: (ESI) *m/z* calculated for $[C_{14}H_{24}NO_4]^+$ 270.17012; found 270.16998. *m/z* calculated for $[C_{14}H_{23}NNaO_4]^+$ 292.15202; found 292.15193.

Compound 28. A 1 M solution of MeONa in dry methanol (408 μL, 0.408 mmol, 0.4 equiv.) was added at room temperature to a solution of compound **27** (284 mg, 0.96 mmol, 1 equiv.) in dry MeOH (8 mL). The mixture was stirred at room temperature. After 1 h TLC monitoring (TLC 2 : 8 Hex : EtOAc R_f (**27**) = 0.5, R_f (**28**) = 0.3 $KMnO_4$ stain) showed total consumption of the starting material. A 2 M solution of $NaHSO_4$ in water (204 μL, 0.408 mmol, 0.4 equiv.) was added. The white precipitate was filtered and washed with MeOH; the organic phase was evaporated to obtain compound **28** (220 mg, quant.), which was used without further purification in the next reaction. ^{1}H NMR (600 MHz, $CDCl_3$) δ 5.97–5.84 (m, 2H, H_1, H_5), 4.54 (s, 1H, NH), 4.51 (d, J_{3-4} = 4.5 Hz, 1H, H_4), 4.38–4.30 (m, 1H, H_2), 3.78 (m, 1H, H_3), 3.30 (quint, J_{9-10} = 5.8 Hz, 1H, H_9), 2.07 (s, 3H, CH_{3NHAc}), 1.56–1.43 (m, 4H, H_{10}), 0.97–0.86 (m, 6H, H_{11}). ^{13}C NMR (150 MHz, $CDCl_3$) δ 172.64 (CO_{Ac}), 134.36 (C_5), 131.87 (C_1), 84.42 (C_4), 81.29 (C_9), 76.95 (C_2), 68.91 (C_3), 26.83 (C_{10}), 26.69 (C_{10}), 23.23 (C_{NHAc}), 9.84 (C_{11}), 9.80 (C_{11}). HRMS: (ESI) *m/z* calculated for $[C_{12}H_{22}NO_3]^+$ 228.15922; found 228.15942. *m/z* calculated for $[C_{12}H_{21}NNaO_3]^+$ 250.14118; found 250.14136. *m/z* calculated for $[C_{12}H_{21}NKO_3]^+$ 266.11486; found 266.11530.

Compound 21. Compound **28** (218 mg, 0.96 mmol, 1 equiv.) was dissolved in dry CH_2Cl_2 (19 mL) under nitrogen atmosphere and Dess–Martin periodinane (813 mg, 1.92 mmol, 2 equiv.) was added in one portion at room temperature. The reaction was stirred until completion (approx. 3 h, TLC 2 : 8 Hex : EtOAc R_f (**28**) = 0.3, R_f (**21**) = 0.4, $KMnO_4$ stain) then quenched with sodium thiosulfate (saturated solution), extracted four times with EtOAc, washed with brine, dried with sodium sulfate, filtered and concentrated under vacuum. The product was purified by column chromatography (from 7 : 3 Hex : EtOAc to 0 : 100 Hex : EtOAc in 15 CV) to yield **21** (183 mg; 86% yield). ^{1}H NMR (500 MHz, $CDCl_3$) δ 7.59 (dd, J_{1-5} = 6.2 Hz, J_{3-5} = 1.9 Hz, 1H, H_5), 6.57 (d, $J_{3\text{-}NH}$ = 6.8 Hz, 1H, NH), 6.44 (dd, J = 6.2 Hz, J_{1-3} = 1.2 Hz, 1H, H_1), 5.00–4.94 (m, 1H, H_4), 3.91 (m, 1H, H_3), 3.56 (quint, J_{9-10} = 5.8 Hz, 1H, H_9), 2.17 (s, 3H, CH_{3NHAc}), 1.74–1.60 (m, 4H, H_{10}), 1.05 (t, J_{10-11} = 7.4 Hz, 6H, H_{11}). ^{13}C NMR (125 MHz, $CDCl_3$) δ 201.30 (C_2), 170.75 (CO_{Ac}), 159.39 (C_1), 133.09 (C_5), 82.44 (C_4), 80.34 (C_9), 63.37 (C_3), 26.57 (C_{10}), 26.17 (C_{10}), 22.91 (C_{NHAc}), 9.74 (C_{11}), 9.60 (C_{11}). HRMS: (ESI) *m/z* calculated for $[C_{12}H_{20}NO_3]^+$ 226.14379; found 226.14377. *m/z* calculated for $[C_{12}H_{19}NNaO_3]^+$ 248.12587; found 248.12571.

Compounds 20 and 30. To a suspension of ethyl (dimethylsulfonium) acetate bromide **29** (240 mg, 1.036 mmol, 1.2 equiv.) in $CHCl_3$ (5 mL), DBU (155 μL, 1.036 mmol, 1.2 equiv.) was added. The resulting suspension was stirred vigorously at room temperature for 30 min. Compound **21** (195 mg, 0.863 mmol, 1 equiv.) was dissolved in $CHCl_3$ (5 mL) and added to the stirring mixture. The reaction mixture was stirred overnight at room temperature. (TLC 2 : 8 Hex : EtOAc R_f (**21**) = 0.3, R_f (**30**) = 0.55, R_f (**20**) = 0.71, $KMnO_4$ stain). The reaction mixture was diluted with $CHCl_3$ (10 mL) and washed with

Open Access Article. Published on 07 June 2016. Downloaded on 11/1/2025 4:50:22 AM.
This article is licensed under a Creative Commons Attribution-NonCommercial 3.0 Unported Licence.

0.1 M $NaHSO_4$, dried over sodium sulfate, filtered, and concentrated under vacuum. The residue was purified by column chromatography (from 70 : 30 Hex : EtOAc to 25 : 75 Hex : EtOAc in 20 CV) to yield **20** (87 mg; 32% isolated yield) and 90 mg of a fraction containing **30** and other impurities. This fraction was subjected to a second purification (from 100 : 0 $CHCl_3$: MeOH to 92 : 8 $CHCl_3$: MeOH in 13 CV) to afford pure **30** (77 mg; 30% isolated yield). Compound **20** ^{1}H NMR (600 MHz, acetone-d6) δ 7.44 (d, $J_{3\text{-}NH}$ = 7.7 Hz, 1H, NH), 4.51 (dd, J_{3-4} = 7.5 Hz, J_{4-5} = 5.1 Hz, 1H, H_4), 4.19–4.10 (m, 2H, CH_{2Et}), 3.86 (t, J = 7.6 Hz, 1H, H_3), 3.42 (m, 1H, H_9), 2.71 (ddd, J_{1-5} = 6.2 Hz, J_{4-5} = 5.1 Hz, J_{5-6} = 3.6 Hz, 1H, H_5), 2.56 (t, J = 3.1 Hz, 1H, H_6), 2.31 (ddd, J_{1-5} = 6.2 Hz, J_{1-6} = 2.7 Hz, 0.8 Hz, 1H, H_1), 1.90 (s, 3H, CH_{3NHAc}), 1.57–1.42 (m, 4H, H_{10}), 1.24 (t, J = 7.1 Hz, 3H, CH_{3Et}), 0.93 (t, J_{10-11} = 7.4 Hz, 3H, H_{11}), 0.87 (t, J = 7.4 Hz, 3H, H_{11}). ^{13}C NMR (150 MHz, acetone-d6) δ 202.62 (C_2), 170.69 (CO_{Et}), 169.98 (CO_{Ac}), 81.22 (C_9), 77.08 (C_4), 61.75 (CH_{2Et}), 58.65 (C_3), 36.23 (C_1), 31.45 (C_5), 27.39 (C_{10}), 27.23 (C_{10}), 24.88 (C_6), 22.56 (C_{Ac}), 14.46 (CH_{3Et}), 10.19 (C_{11}), 9.68 (C_{11}). HRMS: (ESI) m/z calculated for $[C_{16}H_{26}NO_5]^+$ 312.18085; found 312.18054. m/z calculated for $[C_{16}H_{25}NNaO_5]^+$ 334.16318; found 334.16249. Compound **30** ^{1}H NMR (600 MHz, $CDCl_3$) δ 5.75 (d, $J_{3\text{-}NH}$ = 8.0 Hz, 1H, NH), 4.43 (dd, J = 8.0 Hz, J_{3-4} = 5.1 Hz, 1H, H_3), 4.25 (d, J = 5.1 Hz, 1H, H_4), 4.17 (q, J = 7.1 Hz, 2H, CH_{2Et}), 3.38–3.31 (m, 1H, H_9), 2.64 (dd, J_{1-5} = 6.1 Hz, J_{5-6} = 3.8 Hz, 1H, H_5), 2.38 (dd, J = 3.8 Hz, J_{1-6} = 2.5 Hz, 1H, H_6), 2.34 (dd, J = 6.1, 2.5 Hz, 1H, H_1), 2.04 (s, 3H, CH_{3NHAc}), 1.59–1.41 (m, 4H, H_{10}), 1.28 (t, J = 7.1 Hz, 3H, CH_{3Et}), 0.90 (t, J_{10-11} = 7.4 Hz, 3H, H_{11}), 0.85 (t, J = 7.4 Hz, 3H, H_{11}). ^{13}C NMR (150 MHz, $CDCl_3$) δ 205.73 (C_2), 170.27 (CO_{Ac}), 169.32 (CO_{Et}), 81.61 (C_9), 72.53 (C_4), 61.73 (CH_{2Et}), 53.62 (C_3), 33.07 (C_5), 31.50 (C_1), 26.30 (C_{10}), 26.12 (C_6), 25.78 (C_{10}), 22.99 (C_{Ac}), 14.13 (CH_{3Et}), 9.76 (C_{11}), 9.24 (C_{11}). HRMS: (ESI) m/z calculated for $[C_{16}H_{26}NO_5]^+$ 312.18085; found 312.18055. m/z calculated for $[C_{16}H_{25}NNaO_5]^+$ 334.16318; found 334.16249.

Compound 35. Compound **20** (87 mg, 0.279 mmol, 1 equiv.) was dissolved in MeOH (2 mL) and 450 mg of the borohydride (polymer-supported on Amberlite IRA-400, 2.5 mmol g^{-1} resin) were added in one portion at room temperature. The reaction was stirred until completion (2 h; TLC 2 : 8 Hex : EtOAc R_f (**20**) = 0.71, R_f (**35**) = 0.12, $KMnO_4$ stain), then filtered. The resin was washed with MeOH and the solution concentrated under vacuum. The product was purified by column chromatography (from 90 : 10 Hex : EtOAc to 0 : 100 Hex : EtOAc in 8 CV, then 0 : 100 Hex : EtOAc for 5 CV) to yield **35** (80 mg; 91% yield). ^{1}H NMR (600 MHz, $CDCl_3$) δ 5.63 (bs, 1H, NH), 5.11 (s, 1H, OH), 4.24 (dd, J_{1-2} = 6.6 Hz, J_{2-3} = 3.2 Hz, 1H, H_2), 4.18–4.06 (m, 2H, CH_{2Et}), 4.04 (dd, J_{3-4} = 7.6 Hz, J_{4-5} = 4.2 Hz, 1H, H_4), 3.32–3.25 (m, 1H, H_9), 3.25 (td, J = 7.6 Hz, 3.2 Hz, 1H, H_3), 2.25–2.13 (m, 2H, H_6, H_1), 2.15 (dt, J_{1-5} = 6.7 Hz, 4.2 Hz, 1H, H_5), 2.02 (s, 3H, CH_{3NHAc}), 1.59–1.40 (m, 4H, H_{10}), 1.24 (t, J = 7.1 Hz, 3H, CH_{3Et}), 0.91 (dt, J = 16.7, J_{10-11} = 7.4 Hz, 6H, H_{11}). ^{13}C NMR (150 MHz, $CDCl_3$) δ 173.13 (CO_{Ac}), 172.73 (CO_{Et}), 80.77 (C_9), 79.50 (C_4), 74.71 (C_2), 62.10 (C_3), 60.89 (CH_{2Et}), 30.14 (C_1), 28.48 (C_5), 26.98 (C_{10}), 26.28 (C_{10}), 23.20 (C_{Ac}), 18.85 (C_6), 14.35 (CH_{3Et}), 10.01 (C_{11}), 9.69 (C_{11}). HRMS: (ESI) m/z calculated for $[C_{16}H_{28}NO_5]^+$ 314.19495; found 314.19425. m/z calculated for $[C_{16}H_{27}NNaO_5]^+$ 336.17681; found 336.17833.

Compound 13. Compound **35** (10 mg, 0.032 mmol, 1 equiv.) was dissolved in MeOH (260 μL) and H_2O (40 μL) at 0 °C. Next, 20 μL of a solution of NaOH (400 mg in 1.4 mL of H_2O) was added and the mixture was kept at 4 °C overnight. The solution was diluted with water (5 mL) and extracted once with EtOAc (10 mL). The water layer was acidified with 0.5 M HCl and extracted with EtOAc (3 × 10 mL). Organic extracts were dried over sodium sulfate, evaporated at reduced pressure. Dissolution in $CDCl_3$ for NMR analysis led to formation of a white precipitate, which was filtered to afford pure compound **13** (4 mg; 44% isolated yield). ^{1}H NMR (500 MHz, D_2O) δ 4.22 (dd, J_{2-3} = 8.0 Hz, J_{1-2} = 4.4 Hz, 1H, H_2), 4.17 (dd, J_{3-4} = 8.1 Hz, J_{4-5} = 4.4 Hz, 1H, H_4), 3.60 (t, J = 8.1 Hz, 1H, H_3), 3.40 (quint, J_{9-10} = 6.0 Hz, 1H, H_9), 2.28 (dt, J_{1-5} = 7.2 Hz, J_{5-6} = 3.7 Hz, 1H, H_5), 2.23–2.16 (m, 2H, H_1, H_6), 2.00 (s, 3H, CH_{3NHAc}), 1.59–1.37 (m, 4H, H_{10}), 0.89 (t, J_{10-11} = 7.4 Hz, 3H, H_{11}), 0.83 (t, J = 7.4 Hz, 3H, H_{11}). ^{13}C NMR (150 MHz, D_2O) δ 177.05 (CO_{Ac}), 174.12 (CO_{COOH}), 82.98 (C_9), 79.03 (C_4), 73.14 (C_2), 56.78 (C_3), 29.48 (C_1), 28.47 (C_5), 26.17 (C_{10}), 26.13 (C_{10}), 22.08 (C_6), 18.50 (C_{Ac}), 9.01 (C_{11}), 8.71 (C_{11}). HRMS: (ESI) m/z calculated for $[C_{14}H_{24}NO_5]^+$ 286.16614; found 286.16490. m/z calculated for $[C_{14}H_{23}NNaO_5]^+$ 308.14787; found 308.14684. m/z calculated for $[C_{14}H_{23}NKO_5]^+$ 324.12206; found 324.12078.

Compounds 36 and 37. Compound **30** (38 mg, 0.122 mmol, 1 equiv.) was dissolved in MeOH (2 mL) and 260 mg of the borohydride (polymer-supported on Amberlite IRA-400, 2.5 mmol g^{-1} resin) were added in one portion at room temperature. The reaction was stirred until completion (2 h; TLC 2 : 8 Hex : EtOAc, R_f (**30**) = 0.55, R_f (**36**) = 0.33, R_f (**37**) = 0.42, $KMnO_4$ stain), then filtered. The resin was washed with MeOH and the solution concentrated and dried under vacuum. The residue was purified by column chromatography (from 100 : 0 $CHCl_3$: MeOH to 97 : 3 $CHCl_3$: MeOH in 25 CV) to afford pure **36** (13 mg; 34% isolated yield) and **37** (8 mg; 21% isolated yield). Compound **36** ^{1}H NMR (600 MHz, $CDCl_3$) δ 6.08 (d, $J_{3\text{-}NH}$ = 8.2 Hz, 1H, NH), 4.15–4.08 (m, 2H, CH_{2Et}), 4.01 (dd, $J_{2\text{-}OH}$ = 9.6 Hz, J_{2-3} = 3.9 Hz, 1H, H_2), 3.96 (d, J_{3-4} = 4.4 Hz, 1H, H_4), 3.80–3.73 (m, 1H, H_3), 3.30 (quimt, J_{9-10} = 5.6 Hz, 1H, H_9), 2.18 (dd, J_{1-5} = 6.4 Hz, J_{5-6} = 2.9 Hz, 1H, H_5), 2.15 (dd, J = 6.4 Hz, J_{1-6} = 3.1 Hz, 1H, H_1), 2.10 (d, J = 9.6 Hz, 1H, OH), 2.00 (s, 3H, CH_{3NHAc}), 1.59 (t, J = 3.0 Hz, 1H, H_6), 1.57–1.44 (m, 4H, H_{10}), 1.25 (t, J = 7.1 Hz, 3H, CH_{3Et}), 0.92 (t, J_{10-11} = 7.4 Hz, 3H, H_{11}), 0.86 (t, J = 7.5 Hz, 3H, H_{11}). ^{13}C NMR (150 MHz, $CDCl_3$) δ 171.70 (CO_{Ac}), 170.03 (CO_{Et}), 82.08 (C_9), 76.83 (C_4), 72.60 (C_2), 61.12 (CH_{2Et}), 52.50 (C_3), 31.58 (C_1), 30.24 (C_5), 26.48 (C_{10}), 25.82 (C_{10}), 23.36 (C_{Ac}), 21.34 (C_6), 14.30 (CH_{3Et}), 10.01 (C_{11}), 9.42 (C_{11}). HRMS: (ESI) m/z calculated for $[C_{16}H_{28}NO_5]^+$ 314.19495; found 314.19620. Compound **37** ^{1}H NMR (600 MHz, $CDCl_3$) δ 6.33 (d, $J_{3\text{-}NH}$ = 5.6 Hz, 1H, NH), 4.42 (dd, J_{2-3} = 7.1 Hz, J_{1-2} = 4.6 Hz, 1H, H_2), 4.11 (qd, J = 7.1, 2.8 Hz, 2H, CH_{2Et}), 4.01 (d, J_{3-4} = 5.9 Hz, 1H, H_4), 3.60–3.66 (m, 1H, H_3), 3.38–3.32 (m, 1H, H_9), 2.25 (ddd, J_{1-5} = 6.7 Hz, J_{1-2} = 4.6 Hz, J_{1-6} = 3.1 Hz, 1H, H_1), 2.07 (dd, J = 6.7 Hz, J_{5-6} = 3.1 Hz, 1H, H_5), 2.01 (s, 3H, CH_{3NHAc}), 1.91 (t, J = 3.1 Hz, 1H, H_6),

Open Access Article. Published on 07 June 2016. Downloaded on 11/1/2025 4:50:22 AM.
This article is licensed under a Creative Commons Attribution-NonCommercial 3.0 Unported Licence.

1.61–1.46 (m, 4H, H_{10}), 1.25 (t, J = 7.1 Hz, 3H, CH_{3Et}), 0.94 (t, J_{10-11} = 7.4 Hz, 3H, H_{11}), 0.91 (t, J = 7.5 Hz, 3H, H_{11}). ^{13}C NMR (150 MHz, $CDCl_3$) δ 172.41 (CO_{Ac}), 172.38 (CO_{Et}), 81.41 (C_9), 76.17 (C_4), 76.84 (C_2), 61.00 (CH_{2Et}), 58.60 (C_3), 31.61 (C_1), 29.97 (C_5), 26.74 (C_{10}), 25.84 (C_{10}), 23.11 (C_{Ac}), 20.13 (C_6), 14.34 (CH_{3Et}), 10.10 (C_{11}), 9.56 (C_{11}). HRMS: (ESI) m/z calculated for $[C_{16}H_{28}NO_5]^+$ 314.19495; found 314.19620. m/z calculated for $[C_{16}H_{27}NNaO_5]^+$ 336.17681; found 336.17814.

Compound 14. Compound **36** (8 mg, 0.025 mmol, 1 equiv.) was dissolved in MeOH (260 μL) and H_2O (40 μL) at 0 °C. Next, 20 μL of a solution of NaOH (400 mg in 1.4 mL of H_2O) was added and the mixture was kept at 4 °C overnight. The solution was diluted with water (5 mL) and extracted with EtOAc (10 mL). The water layer was acidified with 0.5 M HCl and extracted with EtOAc (3 × 10 mL). Organic extracts were dried over sodium sulfate, evaporated at reduced pressure. Addition of $CHCl_3$ led to formation of a white precipitate, which was filtered to afford pure compound **14** (6 mg; 84% isolated yield). ^{1}H NMR (600 MHz, CD_3OD) δ 7.15–7.10 (m, NH), 4.08 (d, J_{2-3} = 5.0 Hz, 1H, H_2), 3.96 (d, J_{3-4} = 5.4 Hz, 1H, H_4), 3.90–3.84 (m, 1H, H_3), 3.35–3.29 (m, 1H, H_9), 2.16 (dd, J_{1-5} = 6.3 Hz, J_{1-6} = 2.9 Hz, 1H, H_1), 2.10 (dd, J = 6.3 Hz, J_{5-6} = 2.9 Hz, 1H, H_5), 2.03 (s, 3H, CH_{3NHAc}), 1.64–1.51 (m, 4H, H_{10}), 1.52–1.46 (m, 1H, H_6), 1.00 (t, J_{10-11} = 7.4 Hz, 3H, H_{11}), 0.93 (t, J = 7.5 Hz, 3H, H_{11}). ^{13}C NMR (150 MHz, CD_3OD) δ 175.48 (CO_{COOH}), 172.87 (CO_{Ac}), 83.61 (C_9), 78.18 (C_4), 72.24 (C_2), 54.64 (C_3), 33.39 (C_1), 32.10 (C_5), 27.33 (C_{10}), 26.94 (C_{10}), 22.71 (C_{Ac}), 21.51 (C_6), 10.26 (C_{11}), 9.84 (C_{11}). HRMS: (ESI) m/z calculated for $[C_{14}H_{24}NO_5]^+$ 286.16614; found 286.16680. m/z calculated for $[C_{14}H_{23}NNaO_5]^+$ 308.14787; found 308.14699.

Compound 15. Compound **37** (8 mg, 0.025 mmol, 1 equiv.) was dissolved in MeOH (260 μL) and H_2O (40 μL) at 0 °C. Next, 20 μL of a solution of NaOH (400 mg in 1.4 mL of H_2O) was added and the mixture was kept at 4 °C overnight. The solution was diluted with water (5 mL) and extracted with EtOAc (10 mL). The water layer was acidified with 0.5 M HCl and extracted with EtOAc (3 × 10 mL). Organic extracts were dried over sodium sulfate, evaporated at reduced pressure. Addition of EtOAc led to formation of a white precipitate, which was filtered to afford pure compound **15** (7 mg; 90% isolated yield). ^{1}H NMR (600 MHz, CD_3OD) δ 4.38 (dd, J_{2-3} = 8.6 Hz, J_{1-2} = 4.4 Hz, 1H, H_2), 3.90 (d, J_{3-4} = 5.3 Hz, 1H, H_4), 3.60 (dd, J = 8.6, 5.3 Hz, 1H, H_3), 3.24–3.19 (m, 1H, H_9), 2.03–1.99 (m, 1H, H_1), 1.93 (dd, J_{1-5} = 6.7 Hz, J_{5-6} = 3.0 Hz, 1H, H_5), 1.91 (s, 3H, CH_{3NHAc}), 1.86 (t, J = 3.0 Hz, 1H, H_6), 1.53–1.34 (m, 4H, H_{10}), 0.89 (t, J_{10-11} = 7.4 Hz, 3H, H_{11}), 0.82 (t, J = 7.4 Hz, 3H, H_{11}). ^{13}C NMR (150 MHz, CD_3OD) δ 176.10 (CO_{COOH}), 173.60 (CO_{Ac}), 82.77 (C_9), 77.08 (C_4), 76.16 (C_2), 57.45 (C_3), 31.48 (C_1), 30.72 (C_5), 27.35 (C_{10}), 26.92 (C_{10}), 22.54 (C_{Ac}), 20.98 (C_6), 10.23 (C_{11}), 9.58 (C_{11}). HRMS: (ESI) m/z calculated for $[C_{14}H_{24}NO_5]^+$ 286.16614; found 286.16683. m/z calculated for $[C_{14}H_{23}NNaO_5]^+$ 308.14787; found 308.14692.

Compound 38. Compound **20** (68 mg, 0.218 mmol, 1 equiv.) and benzylamine (24 μL, 0.218 mmol, 1 equiv.) were mixed in dry THF (80 mL) at room temperature under N_2. Glacial AcOH (13 μL, 0.218 mmol, 1 equiv.) and sodium triacetoxyborohydride (65 mg, 0.305 mmol, 1.4 equiv.) were added, and the mixture was stirred at room temperature for 16 h (TLC 8 : 2 Hex : EtOAc R_f = 0.11, $KMnO_4$ stain). The reaction mixture was diluted with Et_2O and washed twice with an aqueous saturated $NaHCO_3$ solution. The Et_2O extract was dried over Na_2SO_4 and the solution filtered, concentrated and dried under vacuum. The residue was purified by column chromatography (from 5 : 95 Hex : EtOAc to 100 : 0 Hex : EtOAc in 15 CV, then 5 CV 100 : 0 Hex : EtOAc) to afford pure **38** (50 mg; 60% isolated yield). ^{1}H NMR (600 MHz, $CDCl_3$) δ 7.34–7.27 (m, 5H, H_{Bn}, NH_{Bn}), 7.25–7.21 (m, 1H, H_{Bn}), 5.66 (bs, 1H, NHAc), 4.19–4.15 (m, 1H, H_4), 4.15–4.03 (m, 2H, CH_{2Et}), 3.92 (d, J = 13.5 Hz, 1H, CH_{2Bn}), 3.82 (d, J = 13.6 Hz, 1H, CH_{2Bn}), 3.45–3.35 (m, 2H, H_2, H_3), 3.20 (quint, J_{9-10} = 5.7 Hz, 1H, H_9), 2.13–2.06 (m, 2H, H_5, H_6), 2.05–1.99 (m, 1H, H_1), 1.93 (s, 3H, CH_{3NHAc}), 1.49–1.39 (m, 4H, H_{10}), 1.25 (t, J = 7.1 Hz, 3H, CH_{3Et}), 0.88 (t, J_{10-11} = 7.4 Hz, 3H, H_{11}), 0.84 (t, J = 7.4 Hz, 3H, H_{11}). ^{13}C NMR (150 MHz, $CDCl_3$) δ 172.97 (CO_{Ac}), 170.90 (CO_{Et}), 128.57 (C_{Bn}), 128.37 (C_{Bn}), 127.33 (C_{Bn}), 81.27 (C_9), 79.72 (C_4), 60.80 (CH_{2Et}), 60.27 (C_2), 58.50 (C_3), 51.69 (CH_{2Bn}), 28.97 (C_1), 28.73 (C_5), 26.99 (C_{10}), 26.50 (C_{10}), 23.65 (C_{Ac}), 18.66 (C_6), 14.33 (CH_{3Et}), 10.01 (C_{11}), 9.54 (C_{11}). HRMS: (ESI) m/z calculated for $[C_{23}H_{35}N_2O_4]^+$ 403.25919; found 403.25899.

Compound 16. Compound **38** (12 mg, 0.0298 mmol, 1 equiv.) was dissolved in MeOH (200 μL) and H_2O (40 μL) at 0 °C. Next, 15 μL of a solution of NaOH (400 mg in 1.4 mL of H_2O) was added and the mixture was kept at 4 °C overnight. The solution was diluted with water (3 mL), frozen and lyophilized. The white powder was then dissolved in $CHCl_3$ and directly loaded on a silica column for purification (from 98 : 2 $CHCl_3$: MeOH to $CHCl_3$: MeOH in 15 CV) to afford pure **16** (5 mg; 45% isolated yield). ^{1}H NMR (400 MHz, $CDCl_3$) δ 7.41–7.31 (m, 4H, H_{Bn}), 7.26 (m, 1H, H_{Bn}), 5.40 (bs, 1H, NHAc), 4.17 (dd, J_{3-4} = 7.9 Hz, J_{4-5} = 4.2 Hz, 1H, H_4), 3.91 (d, J = 13.7 Hz, 1H, CH_{2Bn}), 3.82 (d, J = 13.7 Hz, 1H, CH_{2Bn}), 3.42–3.31 (m, 2H, H_2, H_3), 3.23 (dt, J = 11.5, 5.7 Hz, 1H, H_9), 2.16–2.08 (m, 2H, H_5, H_6), 2.08–2.04 (m, 1H, H_1), 1.98 (s, 3H, CH_{3NHAc}), 1.43–1.38 (m, 4H, H_{10}), 0.96–0.82 (m, 6H, H_{11}). ^{13}C NMR (125 MHz, $CDCl_3$) δ 173.48 (CO_{COOH}), 170.58 (CO_{Ac}), 140.43 (C_{Bn}), 128.35 (C_{Bn}), 128.02 (C_{Bn}), 126.91 (C_{Bn}), 99.98 (C_{qBn}), 81.06 (C_9), 79.70 (C_4), 60.31 (C_2), 58.71 (C_3), 51.77 (CH_{2Bn}), 29.37 (C_1), 28.83 (C_5), 26.82 (C_{10}), 26.25 (C_{10}), 23.59 (C_{Ac}), 18.21 (C_6), 9.85 (C_{11}), 9.38 (C_{11}). HRMS: (ESI) m/z calculated for $[C_{21}H_{31}N_2O_4]^+$ 375.22828; found 375.22783. m/z calculated for $[C_{21}H_{30}N_2NaO_4]^+$ 397.20975; found 397.20978.

Compound 39. Compound **20** (22 mg, 0.071 mmol, 1 equiv.) and 4-phenyl-benzylamine (13 mg, 0.0707 mmol, 1 equiv.) were mixed in dry THF (80 mL) at room temperature under N_2. Glacial AcOH (4 μL, 0.0707 mmol, 1 equiv.) and sodium triacetoxyborohydride (20 mg, 0.099 mmol, 1.4 equiv.) were added, and the mixture was stirred at room temperature for 16 h (TLC 8 : 2 Hex : EtOAc R_f = 0.21, $KMnO_4$ stain). The reaction mixture was diluted with Et_2O and washed twice with an aqueous saturated $NaHCO_3$ solution. The Et_2O extract was dried over Na_2SO_4 and the solution filtered, concentrated and dried under vacuum. The residue was purified by column chromato-

Open Access Article. Published on 07 June 2016. Downloaded on 11/1/2025 4:50:22 AM.
This article is licensed under a Creative Commons Attribution-NonCommercial 3.0 Unported Licence.

graphy (from 100 : 0 $CHCl_3$: MeOH to 70 : 30 $CHCl_3$: MeOH in 18 CV) to afford pure **39** (20 mg; 59% isolated yield). ^{1}H NMR (400 MHz, $CDCl_3$) δ 7.61–7.50 (m, 4H, Ar-H), 7.48–7.37 (m, 4H, Ar-H), 7.33 (t, J = 7.3 Hz, 1H, Ar-H), 5.47 (bs, 1H, NHAc), 4.21–4.02 (m, 3H, H_4, CH_{2Et}), 3.95 (d, J = 13.7 Hz, 1H, CH_{2Bn}), 3.84 (d, J = 13.7 Hz, 1H, CH_{2Bn}), 3.47–3.32 (m, 2H, H_2, H_3), 3.27–3.17 (m, 1H, H_9), 2.14–2.06 (m, 3H, H_6, H_1, H_5), 1.96 (s, 3H, CH_{3NHAc}), 1.55–1.40 (m, 4H, H_{10}), 1.24 (t, J = 7.1 Hz, 3H, CH_{3Et}), 0.89 (t, J_{10-11} = 7.4 Hz, 3H, H_{11}), 0.85 (t, J = 7.4 Hz, 3H, H_{11}). ^{13}C NMR (150 MHz, $CDCl_3$) δ 173.10 (CO_{Ac}), 170.74 (CO_{Et}), 141.07 (C_{Ar}), 140.09 (C_{Ar}), 128.89 (C_{Ar}), 128.66 (C_{Ar}), 127.32 (C_{Ar}), 127.25 (C_{Ar}), 127.16 (C_{Ar}), 81.22 (C_9), 79.94 (C_4), 60.78 (CH_{2Et}), 60.45 (C_2), 58.86 (C_3), 51.48 (CH_{2Bn}), 28.97 (C_1, C_5), 27.02 (C_{10}), 26.52 (C_{10}), 23.76 (C_{Ac}), 18.66 (C_6), 14.36 (CH_{3Et}), 10.04 (C_{11}), 9.58 (C_{11}). HRMS: (ESI) m/z calculated for $[C_{29}H_{39}N_2O_4]^+$ 479.29247; found 479.29043. m/z calculated for $[C_{29}H_{38}N_2NaO_4]^+$ 501.27266; found 501.27238.

Compound 17. Compound **39** (6 mg, 0.012 mmol, 1 equiv.) was dissolved in MeOH (150 μL) and H_2O (30 μL) at 0 °C. Next, 5 μL of a solution of NaOH (400 mg in 1.4 mL of H_2O) was added and the mixture was kept at 4 °C overnight. The solution was diluted with water (2 mL), frozen, and lyophilized. The white powder was then dissolved in $CHCl_3$ and directly loaded on a silica column for purification (from 98 : 2 $CHCl_3$: MeOH to 70 : 30 $CHCl_3$: MeOH in 12 CV) to afford pure **17** (4 mg; 70% isolated yield). ^{1}H NMR (500 MHz, CD_3OD) δ 7.60 (dd, J = 12.9, 7.8 Hz, 4H, Ar-H), 7.48–7.40 (m, 4H, Ar-H), 7.34 (t, J = 7.4 Hz, 1H, Ar-H), 4.10 (dd, J_{3-4} = 7.3 Hz, J_{4-5} = 4.5 Hz, 1H, H_4), 3.87 (s, 2H, CH_{2Bn}), 3.63 (t, J = 8.2 Hz, 1H, H_3), 3.28–3.20 (m, 2H, H_2, H_9), 2.18 (t, J = 3.0 Hz, 1H, H_6), 2.10 (dt, J_{1-5} = J_{5-4} = 7.3 Hz, J_{5-6} = 3.7 Hz, 1H, H_5), 2.03 (dt, J = 7.3 Hz, J_{1-6} = 3.5 Hz, 1H, H_1), 1.95 (s, 3H, CH_{3NHAc}), 1.55–1.45 (m, 4H, H_{10}), 0.92 (t, J_{10-11} = 7.4 Hz, 3H, H_{11}), 0.88 (t, J = 7.4 Hz, 3H, H_{11}). ^{13}C NMR (150 MHz, CD_3OD) δ 173.62 (CO_{COOH}), 172.11 (CO_{Ac}), 140.74 (C_{Ar}), 139.95 (C_{Ar}), 138.76, 128.48 (C_{Ar}), 128.43 (C_{Ar}), 126.87 (C_{Ar}), 126.61 (C_{Ar}), 126.45 (C_{Ar}), 81.35 (C_9), 80.27 (C_4), 60.56 (C_2), 56.55 (C_3), 50.62 (CH_{2Bn}), 28.71 (C_1), 28.58 (C_5), 26.39 (C_{10}), 25.98 (C_{10}), 21.46 (C_{Ac}), 18.04 (C_6), 8.72 (C_{11}), 8.31 (C_{11}). HRMS: (ESI) m/z calculated for $[C_{27}H_{35}N_2O_4]^+$ 451.26074; found 451.25913. m/z calculated for $[C_{27}H_{34}N_2NaO_4]^+$ 473.24340; found 473.24108.

Competing interest

The authors declare no competing financial interest.

Acknowledgements

The research leading to these results received funding from the People Programme of the European Union's Seventh Framework Programme by a Marie Curie Outgoing Fellowship to C. C. under REA grant agreement no. PIOF-GA-2012-327579. AJB and BMP thank the Canadian Institutes of Health Research for an operating grant (MOP-259122).

References

1 J. Du, T. A. Cross and H. X. Zhou, *Drug Discovery Today*, 2012, **17**, 1111–1120.
2 C. U. Kim, W. Lew, M. A. Williams, H. T. Liu, L. J. Zhang, S. Swaminathan, N. Bischofberger, M. S. Chen, D. B. Mendel, C. Y. Tai, W. G. Laver and R. C. Stevens, *J. Am. Chem. Soc.*, 1997, **119**, 681–690.
3 M. von Itzstein, W. Y. Wu, G. B. Kok, M. S. Pegg, J. C. Dyason, B. Jin, T. V. Phan, M. L. Smythe, H. F. White, S. W. Oliver, P. M. Colman, J. N. Varghese, D. M. Ryan, J. M. Woods, R. C. Bethell, V. J. Hotham, J. M. Cameron and C. R. Penn, *Nature*, 1993, **363**, 418–423.
4 Y. S. Babu, P. Chand, S. Bantia, P. Kotian, A. Dehghani, Y. El-Kattan, T. H. Lin, T. L. Hutchison, A. J. Elliott, C. D. Parker, S. L. Ananth, L. L. Horn, G. W. Laver and J. A. Montgomery, *J. Med. Chem.*, 2000, **43**, 3482–3486.
5 S. Jain and A. M. Fry, *Clin. Infect. Dis.*, 2011, **52**, 707–709.
6 J. L. McKimm-Breschkin, *Influenza Other Respir. Viruses*, 2013, **7**, 25–36.
7 R. J. Russell, L. F. Haire, D. J. Stevens, P. J. Collins, Y. P. Lin, G. M. Blackburn, A. J. Hay, S. J. Gamblin and J. J. Skehel, *Nature*, 2006, **443**, 45–49.
8 S. Rudrawar, J. C. Dyason, M. A. Rameix-Welti, F. J. Rose, P. S. Kerry, R. J. M. Russell, S. van der Werf, R. J. Thomson, N. Naffakh and M. von Itzstein, *Nat. Commun.*, 2010, **1**, 1–7.
9 Y. C. Xie, D. Q. Xu, B. Huang, X. L. Ma, W. B. Qi, F. Y. Shi, X. Y. Liu, Y. J. Zhang and W. F. Xu, *J. Med. Chem.*, 2014, **57**, 8445–8458.
10 S. Mohan, S. McAtamney, T. Haselhorst, M. von Itzstein and B. M. Pinto, *J. Med. Chem.*, 2010, **53**, 7377–7391.
11 R. E. Amaro, R. V. Swift, L. Votapka, W. W. Li, R. C. Walker and R. M. Bush, *Nat. Commun.*, 2011, **2**, 338.
12 K. T. Greenway, E. B. LeGresley and B. M. Pinto, *PLoS One*, 2013, **8**, e59873.
13 R. E. Amaro, X. L. Cheng, I. Ivanov, D. Xu and J. A. McCammon, *J. Am. Chem. Soc.*, 2009, **131**, 4702–4709.
14 Y. Wu, G. R. Qin, F. Gao, Y. Liu, C. J. Vavricka, J. X. Qi, H. L. Jiang, K. Q. Yu and G. F. Gao, *Sci. Rep.*, 2013, **3**, 1551.
15 M. Niikura, N. Bance, S. Mohan and B. M. Pinto, *Antiviral Res.*, 2011, **90**, 160–163.
16 P. S. Kerry, S. Mohan, R. J. M. Russell, N. Bance, M. Niikura and B. M. Pinto, *Sci. Rep.*, 2013, **3**, 2871.
17 P. J. P. Adabala, E. B. LeGresley, N. Bance, M. Niikura and B. M. Pinto, *J. Org. Chem.*, 2013, **78**, 10867–10877.
18 C. A. Mooney, S. A. Johnson, P. T. Hart, L. Q. van Ufford, C. A. M. de Haan, E. E. Moret and N. I. Martin, *J. Med. Chem.*, 2014, **57**, 3154–3160.
19 J. N. Watson, V. Dookhun, T. J. Borgford and A. J. Bennet, *Biochemistry*, 2003, **42**, 12682–12690.
20 A. G. Watts, I. Damager, M. L. Amaya, A. Buschiazzo, P. Alzari, A. C. Frasch and S. G. Withers, *J. Am. Chem. Soc.*, 2003, **125**, 7532–7533.
21 J. Chan, A. R. Lewis, M. Gilbert, M. F. Karwaski and A. J. Bennet, *Nat. Chem. Biol.*, 2010, **6**, 405–407.

 This journal is © The Royal Society of Chemistry 2016

Open Access Article. Published on 07 June 2016. Downloaded on 11/1/2025 4:50:22 AM.
This article is licensed under a Creative Commons Attribution-NonCommercial 3.0 Unported Licence.

22 J. Chan, A. R. Lewis, D. Indurugalla, M. Schur, W. Wakarchuk and A. J. Bennet, *J. Am. Chem. Soc.*, 2012, **134**, 3748–3757.
23 J. Chan, A. Lu and A. J. Bennet, *J. Am. Chem. Soc.*, 2011, **133**, 2989–2997.
24 M. Raab and I. Tvaroska, *J. Mol. Model.*, 2011, **17**, 1445–1456.
25 F. S. Shidmoossavee, J. N. Watson and A. J. Bennet, *J. Am. Chem. Soc.*, 2013, **135**, 13254–13257.
26 K. S. E. Tanaka, G. C. Winters, R. J. Batchelor, F. W. B. Einstein and A. J. Bennet, *J. Am. Chem. Soc.*, 2001, **123**, 998–999.
27 Y. Wang and A. J. Bennet, *Org. Biomol. Chem.*, 2007, **5**, 1731–1738.
28 C. L. White, M. N. Janakiraman, W. G. Laver, C. Philippon, A. Vasella, G. M. Air and M. Luo, *J. Mol. Biol.*, 1995, **245**, 623–634.
29 L. Kaplan, J. W. Pavlik and K. E. Wilzbach, *J. Am. Chem. Soc.*, 1972, **94**, 3283–3284.
30 T. Damiano, D. Morton and A. Nelson, *Org. Biomol. Chem.*, 2007, **5**, 2735–2752.
31 E. A. Acar, F. Glarner and U. Burger, *Helv. Chim. Acta*, 1998, **81**, 1095–1104.
32 F. Glarner, B. Acar, I. Etter, T. Damiano, E. A. Acar, G. Bernardinelli and U. Burger, *Tetrahedron*, 2000, **56**, 4311–4316.
33 R. Ling and P. S. Mariano, *J. Org. Chem.*, 1998, **63**, 6072–6076.
34 R. Ling, M. Yoshida and P. S. Mariano, *J. Org. Chem.*, 1996, **61**, 4439–4449.
35 J. F. Hayes, M. Shipman and H. Twin, *J. Org. Chem.*, 2002, **67**, 935–942.
36 M. J. Eis and B. Ganem, *Tetrahedron Lett.*, 1985, **26**, 1153–1156.
37 J. B. Sweeney, *Chem. Soc. Rev.*, 2002, **31**, 247–258.
38 B. M. Trost and T. Zhang, *Chem. – Eur. J.*, 2011, **17**, 3630–3643.
39 H. Doi, T. Sakai, K. Yamada and K. Tomioka, *Chem. Commun.*, 2004, 1850–1851.
40 M. Karpf and R. Trussardi, *J. Org. Chem.*, 2001, **66**, 2044–2051.
41 S. Lemaireaudoire, M. Savignac, J. P. Genet and J. M. Bernard, *Tetrahedron Lett.*, 1995, **36**, 1267–1270.
42 F. Guibe, *Tetrahedron*, 1998, **54**, 2967–3042.
43 R. Gigg and C. D. Warren, *J. Chem. Soc.*, 1965, 2205–2210.
44 N. Ohmura, A. Nakamura, A. Hamasaki and M. Tokunaga, *Eur. J. Org. Chem.*, 2008, 5042–5045.
45 H. Lebel, J. F. Marcoux, C. Molinaro and A. B. Charette, *Chem. Rev.*, 2003, **103**, 977–1050.
46 J. L. G. Ruano, C. Fajardo, M. R. Martin, W. Midura and M. Mikolajczyk, *Tetrahedron: Asymmetry*, 2004, **15**, 2475–2482.
47 R. Zhang, A. Mamai and J. S. Madalengoitia, *J. Org. Chem.*, 1999, **64**, 547–555.
48 D. Romo and A. I. Meyers, *J. Org. Chem.*, 1992, **57**, 6265–6270.
49 A. Nakazato, T. Kumagai, K. Sakagami, R. Yoshikawa, Y. Suzuki, S. Chaki, H. Ito, T. Taguchi, S. Nakanishi and S. Okuyama, *J. Med. Chem.*, 2000, **43**, 4893–4909.
50 A. F. Abdel-Magid, K. G. Carson, B. D. Harris, C. A. Maryanoff and R. D. Shah, *J. Org. Chem.*, 1996, **61**, 3849–3862.
51 M. S. Pegg and M. Vonitzstein, *Biochem. Mol. Biol. Int.*, 1994, **32**, 851–858.
52 S. Barrett, P. G. Mohr, P. M. Schmidt and J. L. McKimm-Breschkin, *PLoS One*, 2011, 6.
53 M. Z. Wang, C. Y. Tai and D. B. Mendel, *Antimicrob. Agents Chemother.*, 2002, **46**, 3809–3816.
54 S. Newstead, J. N. Watson, T. L. Knoll, A. J. Bennet and G. Taylor, *Biochemistry*, 2005, **44**, 9117–9122.
55 A. Fersht, *Structure and mechanism in protein science : A guide to enzyme catalysis and protein folding*, W.H. Freeman, New York, 1999.
56 M. Potier, L. Mameli, M. Belisle, L. Dallaire and S. B. Melancon, *Anal. Biochem.*, 1979, **94**, 287–296.